NOTICE

The quality of this microform is heavily dependent upon the quality of the original thesis submitted for microfilming. Every effort has been made to ensure the highest quality of reproduction possible.

If pages are missing, contact the university which granted the degree.

Some pages may have indistinct print especially if the original pages were typed with a poor typewriter ribbon or if the university sent us an inferior photocopy.

Reproduction in full or in part of this microform is governed by the Canadian Copyright Act, R.S.C. 1970, c. C-30, and subsequent amendments.

AVIS

La qualité de cette microforme dépend grandement de la qualité de la thèse soumise au microfilmage. Nous avons tout fait pour assurer une qualité supérieure de reproduction.

S'il manque des pages, veuillez communiquer avec l'université qui a conféré le grade.

La qualité d'impression de certaines pages peut laisser à désirer, surtout si les pages originales ont été dactylographiées à l'aide d'un ruban usé ou si l'université nous a fait parvenir une photocopie de qualité inférieure.

La reproduction, même partielle, de cette microforme est soumise à la Loi canadienne sur le droit d'auteur, SRC 1970, c. C-30, et ses amendements subséquents.

Frame Replenishment Coding Over Noisy Channels

by
Liping Zhang

A THESIS
submitted to the School of Graduate Studies and Research
in partial fulfillment of the requirements
for the degree of
MASTER OF APPLIED SCIENCE
in
Electrical Engineering

Ottawa-Carleton Institute for Electrical Engineering
Department of Electrical Engineering
Faculty of Engineering
University of Ottawa

September, 1990

ISBN 0-315-67994-8

UNIVERSITÉ D'OTTAWA
UNIVERSITY OF OTTAWA

Dedicated to my beloved parents and husband

Abstract

Frame replenishment coding techniques have received considerable attention as source coding techniques for image sequence transmission. Previously, most of these source coding problems have been studied under the assumption that the communication channel is noiseless. But in practice channel error may be considerably high resulting in errors in image reconstruction.

In this thesis, we compare the performances of three frame replenishment coding schemes for noiseless and noisy channel transmission. For the noisy channel case, we propose a combined source-channel coding scheme which provides error protection in order to improve the performance. The three frame replenishment coding techniques are: basic frame replenishment coding (BFR) [66], label replenishment coding using vector quantization (LRVQ) [30] and codeword replenishment coding using vector quantization (CWRVQ) [30]. Our simulation results demonstrate that for a noiseless channel, the LRVQ and CWRVQ techniques provide better performance, and tolerance to motion in the picture, compared to BFR technique. However, in the presence of channel noise LRVQ and CWRVQ techniques exhibit high sensitivities, resulting in poor performance. We propose to use a combined source-channel coding technique with three different error protection schemes where the bit rates for the source code and channel code are adjusted so as to minimize the mean square error. Simulation results demonstrate that the three error protection schemes provide a significant improvement in performance for LRVQ and CWRVQ without sacrificing transmission bandwidth.

Acknowledgements

I wish to express my sincere gratitude to my supervisor, Dr. Morris Goldberg, for his patience, constant encouragement and brilliant insights which has led me to the completion of my thesis.

I would like to express my thanks especially to Dr. S. Panchanathan, for his tremendous efforts and valuable guidance throughout the preparation of this thesis.

I would like to thank all my colleagues and friends for their help and encouragement in so many ways that it is not possible to list them here. My special thanks are also due to Dr. Limin Wang for his valuable suggestions and discussions.

I wish to thank the staff of the Department of Electrical Engineering, University of Ottawa for their assistance, help and support.

Finally, I would like to highlight the very special support from my husband G. Yun and my parents. It would not been possible to finish this work without their support.

Contents

List of Figures

List of Tables

Acronyms

AWGN	Additive white Gaussian noise
A/D	Analog-to-digital conversion
BPSK	Binary-Phase-Shift-Keyed modulation
BSC	Binary symmetric channel
TC	Transform coding
DPCM	Differential PCM
PCM	Phase modulator
VQ	Vector quantization
BFR	Basic conditional frame replenishment coding
BFR-map	Frame replenishment coding using map as the indication of the change
BFR-add	Frame replenishment coding using address as the indication of the change
LRVQ	Label replenishment coding by using vector quantization
LRVQ-map	Label replenishment coding by using vector quantization and using map as the indication of the change
LRVQ-add	Label replenishment coding by using vector quantization and using address as the indication of the change

CWRVQ	Codeword replenishment coding by using vector quantization
CWRVQ-map	Codeword replenishment coding by using vector quantization and using map as the indication of the change
CWRVQ-add	Codeword replenishment coding by using vector quantization and using address as the indication of the change
DCT	Discrete cosine transform
E_b	Signal energy per transmitted binary channel symbol
e^2_{ms}	The total mean squared reconstruction error
ε_q	The mean-squared value of the quantization noise normalized on a per pixel basis
ε_c	The mean-squared error due to channel errors normalized on a per pixel basis
ε_m	The mean-squared mutual error due to the interaction of quantization and channel errors normalized on a per pixel basis
σ^2_s	The variance of the zero-mean stationary sequence
FT	Fourier transform
HT	Hadamard transform
MSE	Mean squared error
NMSE	Normalized mean squared error
NTSC	National television systems committee
n(i,j,k)	Channel errors
n(t)	Gaussian random process
$N_0/2$	Double-sided noise spectral density

Q (.)	Complementary error function of Gaussian statistics
P_b	Bit error probability
R(D)	Rate distortion function.
2-D	Two-dimension
3-D	Three-dimention
$\| \|$	The Norm
r(t)	The received signal
SNR	Signal-to-noise ratio
s	The original image
$\hat{s}$	The reconstructed estimate of original image
s(t)	The transmitted signal
q(i,j,k)	The additive quantization noise associated with the (i,j,k) spatial component
MDC	Minimum distance code.

Chapter 1

Introduction

Image coding, a subfield of data compression, has as objective to reduce the bit rate for transmission or storage while maintaining an acceptable image quality. It has applications in the areas of television transmission, video conferences, transmission of remote sensing images, image data bases, etc. In general, image coding techniques fall into two broad categories, intraframe coding and interframe coding. In interframe coding, both spatial and temporal redundancies are exploited for data compression. Intraframe coding schemes, such as differential pulse-code modulation (DPCM), transform coding have been extended to interframe coding with some modifications [75, 38, 79]. Some coding schemes, for example frame replenishment coding [66], motion-compensated predictive coding [68], are only applied to interframe coding.

The observation that in image sequences a majority of picture elements remain virtually unchanged from frame to frame forms the basis of frame replenishment coding. The conditional (basic) frame replenishment coding technique (BFR) [66] has received considerable attention as a source coding technique for image sequences. In a frame replenishment coder, the first frame of a sequence is stored at the coder as a reference frame and is also transmitted as a reference to the receiver. The subsequent frames are then compared with the reference frame. If the difference is significant, the old pixel value in the frame memory is replaced by the new value, and the new value is transmitted along with its frame address. There are several extensions to the BFR. Frame differences can be coded in clusters to improve the address coding efficiency [10]. Also, further reductions in transmission-rate can be obtained by

subsampling the frame differences in moving image areas [74]. Note that in these techniques the image data is coded using scalar quantization.

Shannon's rate-distortion theory states that it is possible to achieve a better performance by coding vectors instead of scalars. Recently, Goldberg and Sun [30] have extended the replenishment concept to vector quantization (VQ) where replenishment is applied to labels (label replenishment LRVQ) and codewords (codeword replenishment CWRVQ). In vector quantization, the image data to be coded are first processed to yield a set of vectors. Then, a codebook of representative vectors (codewords) is generated. The vectors in the set are then individually quantized to the closest codeword of the codebook. Compression is achieved by replacing the representative vector (codeword) with a label. Reconstruction of the images can be implemented by table lookup techniques; where the label is simply used as an address for a table containing the representative vectors (codewords). In frame replenishment coding techniques using vector quantization, the vectors corresponding to the first frame are taken as the training set for generating the first codebook. Hence, in vector quantization, each vector is encoded by two distinct pieces of information: the label and the corresponding codeword. In encoding subsequent frames, the operation of replenishment can be applied to labels (label replenishment) and codewords (codeword replenishment).

We note that most of the research work on image coding is based on the assumption that the communication channel is noiseless. But in practice, communication channels have significant error probability which may result in errors in signal reconstruction. In such cases, the coding performance cannot be improved by increasing the source coding bit rate [75] [63] [64]. Hence, some error protection must be provided if high-quality image sequence reconstruction is to be achieved [63], [64]. The objective of this thesis is to study the coding performance of three frame replenishment coding techniques (BFR, LRVQ and CWRVQ) over noiseless and noisy channel and then design combined source-channel frame replenishment coding schemes to minimize the distortion of reconstructed images.

The rest of the thesis is organized as follows. Chapter 2 presents a review of image coding

and interframe coding techniques, particularly the three frame replenishment coding schemes [BFR, LRVQ and CWRVQ]. Chapter 3 presents a review on noise effects and error protection techniques for intraframe coding. Chapter 4 compares the performance of the three frame replenishment coding techniques BFR, LRVQ and CWRVQ over noiseless channel. The results of the first set of experiments demonstrate the superior coding performance of LRVQ and CWRVQ techniques in a noiseless channel. Chapter 5 presents the performances of BFR, LRVQ and CWRVQ as regards error propagation and noise effects over noisy channels. The results of this second set of experiments show serious error propagation and noise effects for LRVQ and CWRVQ in a noisy channel. A combined source-channel frame replenishment coding scheme for BFR, LRVQ and CWRVQ with three error protections follows in chapter 6. The results of this third set of experiments demonstrate significant improvement in performance by using combined source-channel coding to LRVQ and CWRVQ. Finally, chapter 7 briefly summarizes the main results, and provides some suggestions for further investigation.

Chapter 2

Review of Image Coding

In this chapter, a short review of digital communication systems is first presented. Distortion measures used in image data compression are then discussed in section 2.2. This is followed by a review of image coding techniques and vector quantization in sections 2.3 and 2.4. Then a review of interframe image coding and three frame replenishment coding techniques used in our thesis are presented in section 2.5 and 2.6 respectively. Finally, a summary is given in section 2.7.

2.1 Model of A Digital Communication System

The basic elements of a digital communications system [58] are illustrated by the block diagram shown in Fig. 2.1. The *information source* generates messages which are to be transmitted to the receiver. The message can be either analog or digital signals. In a digital communication system, the messages produced by the source are usually converted into a sequence of binary digits. The *source encoder or data compressor* transforms the information source into *information sequence* u, a sequence of binary digits (bits). It is necessary for the design of the source encoder (1) that the number of bits per unit time required to represent the source output be minimized, and (2) that the source output can be reconstructed from the information sequence u without ambiguity. The *channel encoder* transforms the information sequence u into a discrete *encoded sequence* v. Discrete symbols are not suitable for trans-

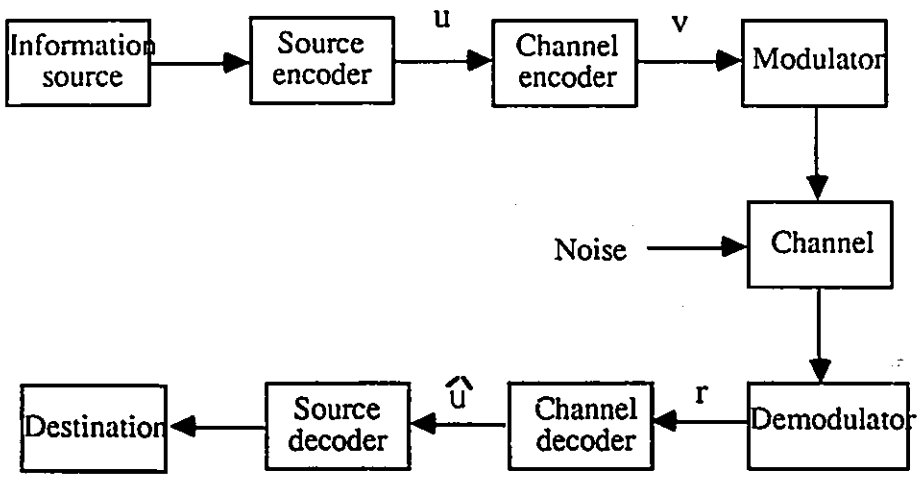

Figure 2.1: Block diagram of a typical digital communications system.

mission over a physical channel, for example a pair of wires, a coaxial cable, an optical fibre channel, a radio channel, a satellite channel, or some combination of these media. Hence, the *modulator* is used to transform each output bit of the channel encoder into a waveform of duration T suitable for transmission. The channel may be subject to various types of noise disturbances and introduce error into the transmitted waveform. The *demodulator* processes each received waveform of duration T and the sequence of demodulator outputs is called the *received sequence* r. The *channel decoder* transforms the received sequence r into a binary sequence û called the *estimated sequence*. The strategy for channel decoding depends upon the channel encoding and the noise characteristics of the channel. Ideally, û will be the same as the information sequence u, however, the noise may result in some *decoding errors* in channel decoding. As a final step, when an analog output is desired, the *source decoder* accepts the output sequence from the channel decoder û and, from knowledge of the source encoding method used, attempts to reconstruct the original signal from the source. Due to channel decoding errors and possible distortion introduced by the source encoder, the signal at the output of the source decoder is an approximation of the original source output.

2.2 Rate Distortion Function

2.2.1 Shannon's rate distortion theory

Shannon's rate distortion function $R(D)$ is a lower bound on the transmission rate required to achieve an average distortion D. The N-block rate distortion function is defined as the minimum of the average mutual information, $I_N(X,Y)$, per pixel:

$$R_N(D^*) = \min_{Q:D(Q)\leq D^*} \frac{1}{N} I_N(X,Y) \tag{2.1}$$

where X is the source input, and Y is the output of the decoder. The limiting value of the N-block rate distortion function is called the *rate distortion funtion*,

$$R(D^*) = \lim_{N\to\infty} R_N(D^*) \tag{2.2}$$

A typical rate distortion function is shown in Fig. 2.2. It is a monotonically non-increasing function. That is, the higher information-rate representations lead to smaller (strictly, non-increasing) average distortion. In practice, the function potentially gives a measure for judging the performance of a coding system. However, this value has not been completely realized for image transmission.

2.2.2 Distortion measures for image coding

Objective distortion measures

The average mean-square error is widely used as a distortion measure of image coding. For an $N\times M$ size image, it is defined as

$$e_{ms}^2 = \frac{1}{NM}\sum_{i=1}^{N}\sum_{j=1}^{M} E(s_{i,j} - \hat{s}_{i,j})^2 \tag{2.3}$$

where $s_{i,j}$ and $\hat{s}_{i,j}$ represent the $N\times M$ original and the reproduced images, respectively. In practice, the average mean-square error is often estimated by the average sample mean-square

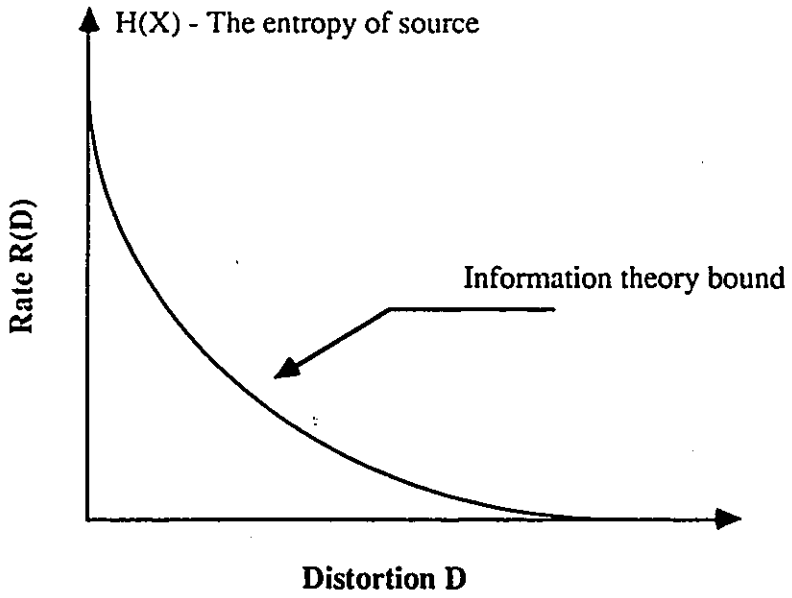

Figure 2.2: Rate distortion function.

error defined by

$$e_{ms}^2 \simeq \frac{1}{NM} \sum_{i=1}^{N} \sum_{j=1}^{M} (s_{i,j} - \hat{s}_{i,j})^2 \tag{2.4}$$

The corresponding signal-to-noise ratio SNR is then defined as,

$$SNR = 10 \log_{10} \frac{\sigma_s^2}{e_{ms}^2} (dB) \tag{2.5}$$

where σ_s^2 is the variance of the original image.

In this thesis, the SNR (in Eq. 2.5) is adopted as the distortion measure for image coding.

Subjective distortion measures

When the images are to be viewed by people, it is more appropriate to use a subjective distortion measure corresponding to how good the images look to observers. Since the human visual system has peculiar characteristics, for example its logarithmic sensitivity to light in-

tensity, two pictures having the same average mean-square error may have different visual qualities. The subjective quality of an image can be rated by showing the image to a number of observers and averaging their evaluations [31].

2.3 Image Coding

Image coding is a specialization of data compression. The goal of image coding is to reduce the bit rate for transmission while maintaining an acceptable fidelity or image quality. Bit compression is achieved by reducing the statistical redundancy and psychophysical redundancy of the image source [75]. A number of image data compression techniques have been developed and they can be broadly classified as lossless and lossy coding techniques.

2.3.1 Lossless coding

The two lossless coding techniques are Huffman coding [43] and run-length coding [40, 62]. In lossless coding, the statistical redundancy of the image is exploited reversely; that is, the original image can be recovered exactly. In Huffman coding, the number of bits for a source sample varies approximately inversely with the corresponding source probability and the coding technique results in a variable length code [47]. In run-length coding, a run, for example, is defined as a sequence of consecutive pixels of identical values along a specified direction. Redundancy reduction is achieved by transmitting the start and length of the run [47].

2.3.2 Lossy coding

The two major lossy coding techniques are predictive coding and transform coding. [31, 75, 37, 80, 47, 68, 46]. In lossy coding, the statistical redundancy of the image is exploited subject to some image quality constraint.

Predictive coding is a technique which has been widely employed for efficient coding of an image [16]. In predictive coding systems, waveform redundancies is utilized in time-domain operations to realize reductions in bit rate. Differential PCM (DPCM) coders, which are based on the notion of quantizing a prediction error signal, are important examples of predictive coding systems [75]. In predictive coding, the pixel value is predicted from the previous pixel $s(n-1)$. The predicted estimate $\hat{s}(n)$ is then subtracted from the actual pixel $s(n)$,

$$d(n) = s(n) - \hat{s}(n) \tag{2.6}$$

and the corresponding difference is quantized, coded, and transmitted. At the decoder, the quantized difference is used to form the reconstructed image. Thus, a predictive coder has three basic components: (1) prediction, (2) quantization, and (3) code assignment.

Transform coding is a popular coding technique for images [3, 77, 79]. In transform coding, the linear dependencies are utilized for efficient digitization, where the image vector V is first linearly transformed using an orthogonal transform $A(A' = A^{-1})$,

$$T = AV \tag{2.7}$$

and the transform coefficients $T_{ij}, i, j = 0, ..., N-1$ are then quantized, Q, with a variable number of bits. At the receiver, the vector, V, of quantized coefficients is inverse transformed to recover the coded image $\hat{I}$, that is,

$$\hat{I} = A'U = A'Q(T) = A'Q(AV) \tag{2.8}$$

The most popular transforms used in transform coding are discrete cosine transform (DCT) [79], Fourier transform (FT) [3] and Hadamard transform (HT) [77]. In designing a transform coder the system block size, the type of transformation, the coefficients to be transmitted, the bit assignment and the quantization strategy must be selected.

The performance of transform coding schemes can be improved by adapting them to changes in image statistics. Three types of adaptation have been developed: namely, (a) adaptation of the transform [91], (b) adaptation of the bit allocation [14] and (c) adaptation

of the quantizer levels [3]. Adaptation of the bit assignment to changes in statistics is the most practical method. By using this method, an image block can be classified into one of several categories and a larger number of bits is allocated to the blocks with larger activity and fewer bits to the blocks with lower activity. Adaptations of this type have been considered by Chen [13] for two dimensional transform coding.

2.4 Vector Quantization

We recall from Shannon's rate-distortion theory that it is possible to obtain a better performance using vector coders instead of scalar coders. Extensive studies of vector quantizers have been performed by many researchers [29, 28, 1, 13, 60]. Reviews of vector quantization are given by Gray [34] and Nasrabadi et al. [49].

A block diagram of the various steps involved in vector quantization, as applied to image coding, is depicted in Fig. 2.3.

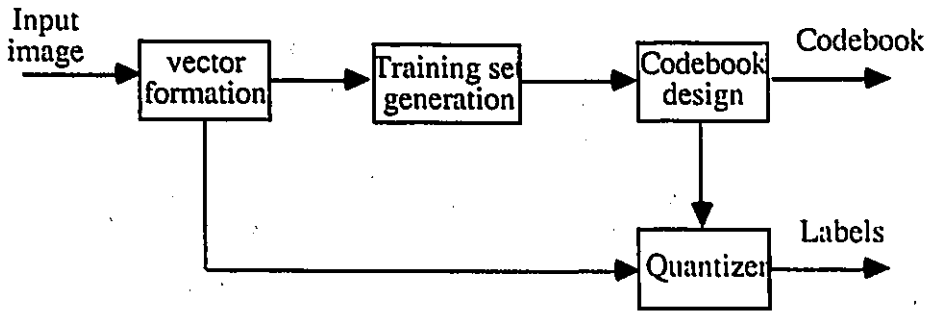

Figure 2.3: A block diagram of vector quantization.

Thus, the design steps in implementing image vector quantization are as follows,

1. **Vector formation:** That is , the decomposition of the images into a set of vectors.
2. **Training set generation:** A training set, representative of the expected input vector source is used to design the vector quantizer.

3. **Codebook generation:** The key step in vector quantization is the development of a good codebook. The optimal codebook, using the mean squared error (MSE) criterion, must satisfy two necessary conditions [28]:

   (a) The input vector source, S, is partitioned into N closed sets or Voronoi regions, $R_i : 1 \leq i \leq N$, with the partition determined by the minimum distance rule:

   $$R_i = \{s : |s - w_i| \leq |s - w_j|\} \qquad j \neq i \tag{2.9}$$

   (b) The corresponding codewords in the codebook are then defined by

   $$w_i = E\{s \mid s \in R_i\} \qquad i = 1, 2, ..., N. \tag{2.10}$$

   The K-means [93] or the closely related generalized Lloyd clustering algorithm proposed by Linde, Buzo, and Gray [59] are typically used to generate the codebook. These algorithms have the advantage of not requiring any knowledge of the underlying statistics of the input source and additionally minimizing a criterion related to the quantization error.

4. **Quantization:** Quantization involves finding the closest codeword for each input vector. Compression is achieved by transmitting the label, L, of the codeword.

5. **Decoding (Q^{-1}):** This is a table look-up procedure.

   $$\hat{V} = Q^{-1}(L) \tag{2.11}$$

   where $\hat{V}$ is the reconstructed vectors, formed from the representative vectors of the codebook.

2.5 Interframe Coding

We note that image coding techniques fall into two general categories, intraframe coding and interframe coding. In interframe coding, both spatial and temporal redundancies are exploited for data compression.

2.5.1 Spatial-temporal domain techniques

Interframe image coding usually involves a combination of spatial and temporal domain techniques. There are two types of interframe predictive coders [23]: frame replenishment [66] and motion compensation [45, 51, 71]. We note that frame replenishment technique is the topic of this thesis. It will be described in further detail in the next section.

In motion compensation interframe coding, the image is regarded as a superposition of moving pixels on a stationary background image. The image is first segmented into stationary and changing areas, and the displacements of moving objects in the changing areas are then estimated. The motion-compensated predictor is then generated by the displacement estimates. Finally the prediction error and side information are coded separately. Compression is achieved by skipping frames on the transmitting side and repeating frames on the receiving side. Approaches to estimating the motion or displacement between successive frames include correlation or matching, and differential techniques [42]. Various motion compensation methods have been proposed, and this is still an area of active research [69].

2.5.2 Three-dimensional transform coding

The basic ideas of the two dimensional transform coding have been extended for compression of three dimensional data. In interframe transform coding, a sequence of image frames $x(k,l,m)$ is transformed in blocks of $K \times L \times M$ pixels. The transform coefficients are

$$T(u,v,w) = \sum_{k=1}^{K} \sum_{l=1}^{L} \sum_{m=1}^{M} x(k,l,m) a(u,v,w;k,l,m), \tag{2.12}$$

where $a(u,v,w;k,l,m)$ is a unitary transform kernel, and (K,L,M) denotes the block size in the row, column and temporal directions. As for intraframe transform coding, compression of data results by selecting a subset of the transform coefficients, which are then quantized and coded for transmission.

2.5.3 Interframe hybrid coding

Hybrid coding is particularly useful in interframe image data compression. In interframe hybrid coding [75], usually, a two dimensional intraframe transform is first performed on spatial blocks within each frame. A linear predictive DPCM coder is then applied in the temporal direction to each resulting transform coefficient.

For three dimensional data, adaptation could be quite useful because the statistical properties along the temporal dimension could vary significantly depending on motion or other temporal changes. The adaptation of the bit assignment to changes in statistics has been considered for three dimensional transform coding [45], in which measures of spatial and temporal activity have been used for adaptive selection and quantization of the coefficients.

2.6 Frame replenishment coding

In an image sequence, successive frames are usually very similar. The interframe coding technique which exploits this similarity is called " conditional frame replenishment coding " [66].

A frame replenishment coder-decoder takes advantage of the considerable similarity between successive frames of image sequence in two ways:

1. The parts of the picture that do not change between frames are not transmitted; at the receiver they are reconstructed simply by repeating the pixel values from the previous frame.

2. The parts with changes in the picture are coded with a varying resolution. The choice of resolution depends on subjective requirements for acceptable picture quality and the bit rate available for transmission.

A number of modifications to the fundamental frame replenishment algorithm [66] have

been proposed. Candy et al. [10] proposed a method of more efficiently addressing the pixels in clusters, instead of individually addressing them. An alternate approach was proposed by Pease and Limb [74] in which the pixels in the changing areas are subsampled by 2:1 along the horizontal direction. Certain studies [68, 74] have demonstrated that the pixels in the changing areas need not be transmitted independently, and can be coded by linear predictive coding. Goldberg and Sun [30] introduced the replenishment concept to vector quantization and proposed two frame replenishment coding techniques using vector quantization: label replenishment coding (LRVQ) and codebook replenishment coding (CWRVQ).

2.6.1 The basic frame replenishment coding (BFR)

The basic frame replenishment coding (BFR) developed by Mounts [66] and subsequently refined by Candy, Haskell, Limb, Pease *et al.* [74, 10, 57, 38] is based on a simple method of detecting and encoding the changing areas which are replenished from frame to frame. In this scheme, only the information necessary to describe the new gray values of the pixels that change between successive frames is transmitted. The implementation uses two frame memories, one at the receiver and another at the transmitter to store the required reference frames. The interframe difference signal is

$$e(i,j,k) = s(i,j,k) - \hat{s}(i,j,k-1) \tag{2.13}$$

where $s(i,j,k)$ denotes the pixel at location (i,j) in frame k, and $\hat{s}(i,j,k-1)$ is the reference frame value corresponding to $s(i,j,k-1)$, i.e., at the $(k-1)$-th frame. If the magnitude of $e(i,j,k)$ is greater than a predetermined threshold η, then it is quantized and coded for transmission. At the receiver, a pixel is reconstructed either by repeating the value of that pixel location from the previous frame, or is replenished by the decoded difference signal,

$$\hat{s}(i,j,k) = \begin{cases} \hat{s}(i,j,k-1) + \hat{e}(i,j,k) & \text{if } |e(i,j,k)| > \eta, \\ \hat{s}(i,j,k-1) & \text{otherwise.} \end{cases}$$

In transmission, codewords representing the quantized values and their addresses are generated. The average bit rate depends on the extent and duration of changes which implies that

a reasonably sized buffer with an appropriate buffer control strategy is necessary to achieve a steady bit rate and to reduce the chance of buffer overflow. A common scheme of buffer control is to raise the threshold whenever the overflow is imminent.

2.6.2 Frame replenishment coding using vector quantization (LRVQ and CWRVQ)

Vector quantization can also be applied to the coding of image sequences. In an extension of the frame replenishment concept, the change in corresponding pixel values between consecutive frames can be coded by updating (replenishing) both the frame label map L and the codebook W [30]. The basic steps of label replenishment and codebook replenishment shown in Fig. 2.4 are as follows,

- The vectors drawn from the first frame V^1 are used to generate a codebook W^1 , and this codebook is then used to quantize the first frame

$$W^1 = G(V^1). \tag{2.14}$$

  The resulting labels L^1 are stored in a frame label map at both the receiver and transmitter

$$L^1 = Q_L^1(V^1). \tag{2.15}$$

- In label replenishment [Fig. 2.4(a)], the second and subsequent frames are quantized with the codebook W^1

$$L^j = Q_L^1(V^1), \qquad j > 1. \tag{2.16}$$

  The resultant labels L^j are then compared to those in the label frame memory L^{j-1}. If there is a change, the new label value is transmitted and both label maps updated; an operation represented by $U(L^j, L^{j-1})$.

- In codeword replenishment [Fig. 2.4(b)], the vectors of the second and subsequent frames $(j > 1)$ are used as a training set to generate a new codebook W^j; however, to ensure

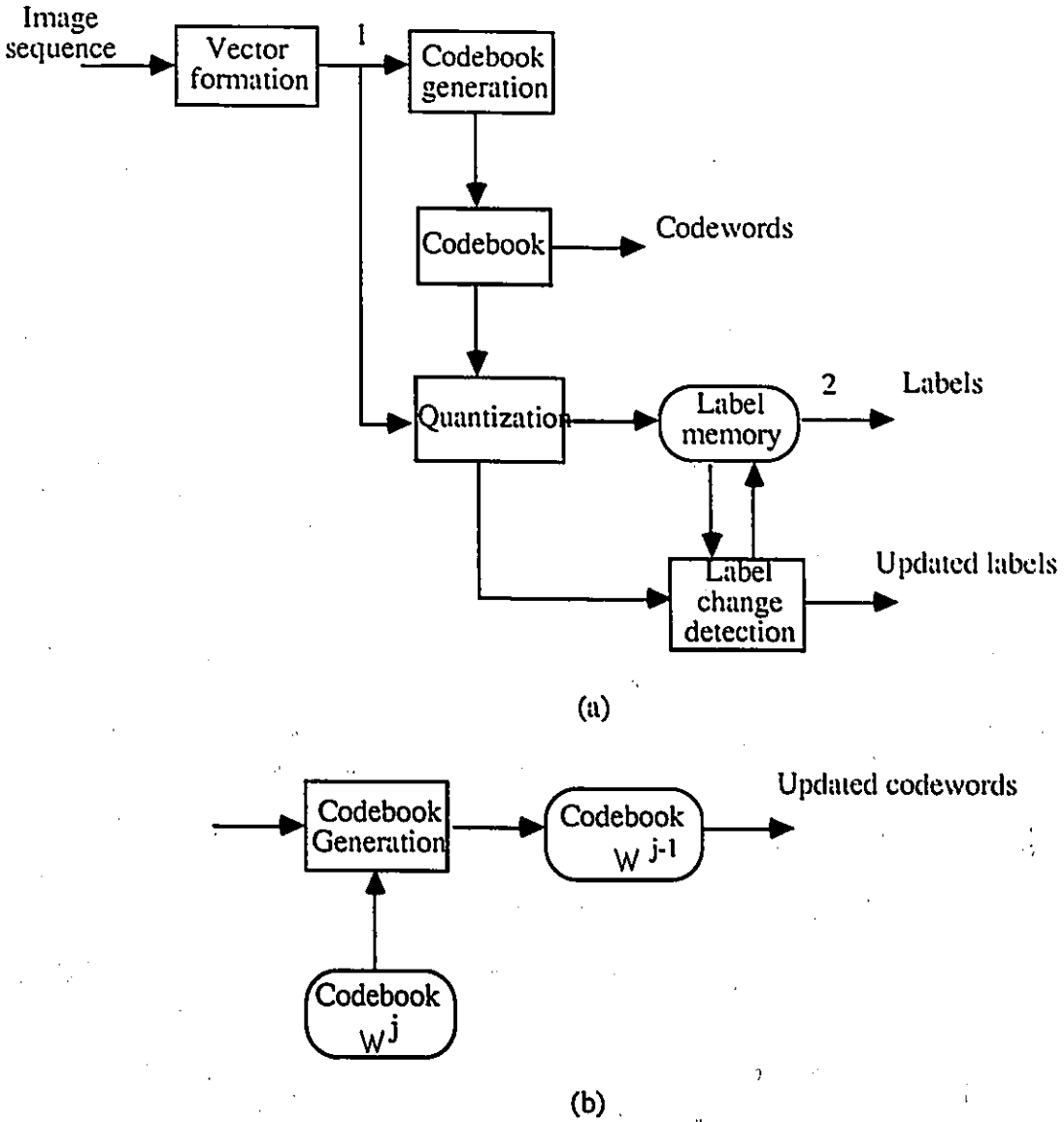

Figure 2.4: (a) Block diagram of label replenishment coding using vector quantization. The line 1 correspond to the codebook generation step using the first frame. The remaining lines correspond to coding of the subsequent frames. (b) Block diagram of codebook replenishment (updating) coding using vector quantization [88].

correlation between the new and old codebooks, the old codebook W^{j-1} is used as initial seeds in the iterative clustering algorithm

$$W^j = G(V^j, W^{j-1}). \qquad j > 1. \tag{2.17}$$

The codebooks are then updated at the receiver and the transmitter; which we represent by $U(W^j, W^{j-1})$. The new codebook is then used to quantize the second frame:

$$L^j = Q_L^j(V^j). \qquad j > 1. \tag{2.18}$$

and label frame replenishment $U(L^j, L^{j-1})$ takes place as required.

According to the label replenishment algorithm presented above, changes in the input source are tracked by only transmitting the changed label components. Thus, only new labels need to be transmitted. The main drawback with this approach is that a codebook which is representative of the entire sequence must be found [88]. Furthermore, if the individual frames have different statistics, then a comparatively large codebook is required, hence increasing the bit rate. An alternative strategy would be, therefore, to design a codebook which tracks the local frame statistics [8]. It is the principal idea behind the codeword replenishment algorithm in which the codebook is replenished by updating the individual representative vectors.

2.7 Summary

In this chapter, we first reviewed digital communication systems. Secondly, various distortion measures, including Shannon's rate distortion theory, objective and subjective distortion measures used in the image data compression were presented. Lossless coding techniques such as, Huffman and run length coding were then discussed. A discussion of lossy coding techniques such as, predictive coding and transform coding is followed. A review of vector quantization as applied to image coding was then presented. Finally, three frame replenishment coding techniques used in this thesis, namely, BFR, LRVQ and CWRVQ, were introduced in detail. BFR is a basic frame replenishment coding proposed by Mounts [66], LRVQ and CWRVQ are

frame replenishment coding techniques using vector quantization proposed by Goldberg and Sun [30].

Chapter 3

Error Protection Techniques for Intraframe Image Transmission

We note that most of the source coding problems, have been studied under the assumption that the communication channel is noiseless. But in practice channel errors may arise and result in errors to the reconstructed images. In such cases, some error protection should be provided to combat channel noise effects. The objective of this chapter is to give a short review of noise effects as well as some protection techniques for intraframe coding techniques. In section 3.1 the effect of channel error on some intraframe coding techniques is presented. This is followed in section 3.2 by a discussion on the techniques used to protect channel errors for intraframe image transmission. Finally, a summary is presented in section 3.3.

3.1 Error Effect on Intraframe Image Transmission

Several studies have been conducted to study the effect of channel errors on the performance of source coders [11, 4, 24, 98, 94]. Generally, channel transmission errors have much stronger effects in DPCM, transform coding and vector quantization systems than in conventional PCM systems.

3.1.1 PCM monochrome image coding channel error effects

An example of PCM channel error effects for monochrome images is shown in Fig. 3.1. PCM channel errors are often described as " salt and pepper" noise because of the discrete appearance of erroneous black pixels in white areas and white pixels in black areas. Subjectively, PCM channel errors are usually tolerable up to error rates of 10^{-3} [76].

Figure 3.1: Channel error effects for PCM image coding at three bit error rates.

3.1.2 Two dimensional DPCM image coding channel error effects

The effect of a transmission error differs from PCM to DPCM. In the PCM the erroneous pixel is perceived as a spot on the image, whereas in DPCM [see Fig. 3.2] [76], the pixel value is predicted from the previous pixels $s(n-1)$. The predicted estimate $\hat{s}(n)$ is then subtracted from the actual pixel $s(n)$

$$d(n) = s(n) - \hat{s}(n) \tag{3.1}$$

and the corresponding difference is quantized, coded, and transmitted. At the decoder, the quantized difference is used to form the reconstructed image. Therefore, if a channel error occurs, the next reconstructed pixel will be in error, and this error will be introduced in all

the subsequent receiver prediction estimates. As a consequence, channel error effects persist along lines of the image until they are corrected.

Modestino and Daut [63] show that in DPCM the reconstructed image quality in noisy channels could not be improved by increasing the quantization accuracy [see Fig. 3.3].

Figure 3.2: Channel error effects for DPCM image coding at 3 bits/pixel. (a) bit error rate $= 10^{-4}$. (b) bit error rate $= 10^{-2}$.

3.1.3 Two dimensional transform image coding channel error effects

We recall from chapter 2 that in a TC system each signal block is linearly transformed into a set of transform coefficients. These coefficients are then quantized independently, transmitted, and transformed back to the spatial domain. Therefore, a single error in one of the transform coefficients of the block leads to errors in all the data samples reconstructed from it. Fig. 3.4 illustrates the effect of channel errors for transform coding [76],

Note that in TC, it is shown [64] that the reconstructed image quality in a noisy channel cannot be improved by increasing the quantization accuracy.

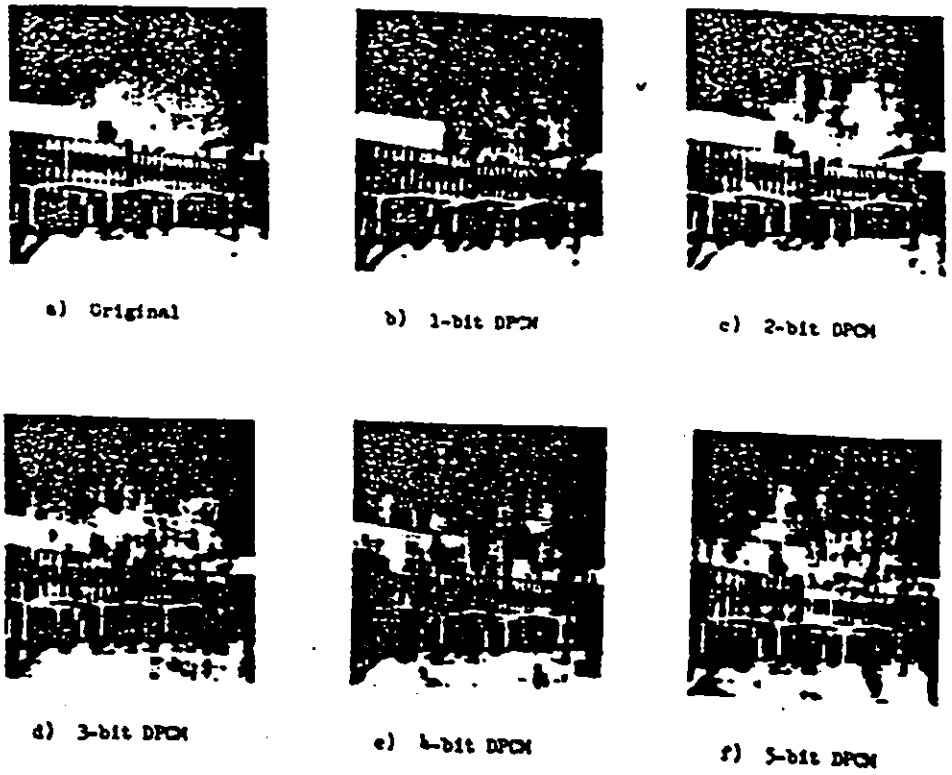

Figure 3.3: Channel error effects on two dimentional DPCM image decoding with different bit rates. Typical outdoor scene; $P_b = 5 \times 10^{-3}$.

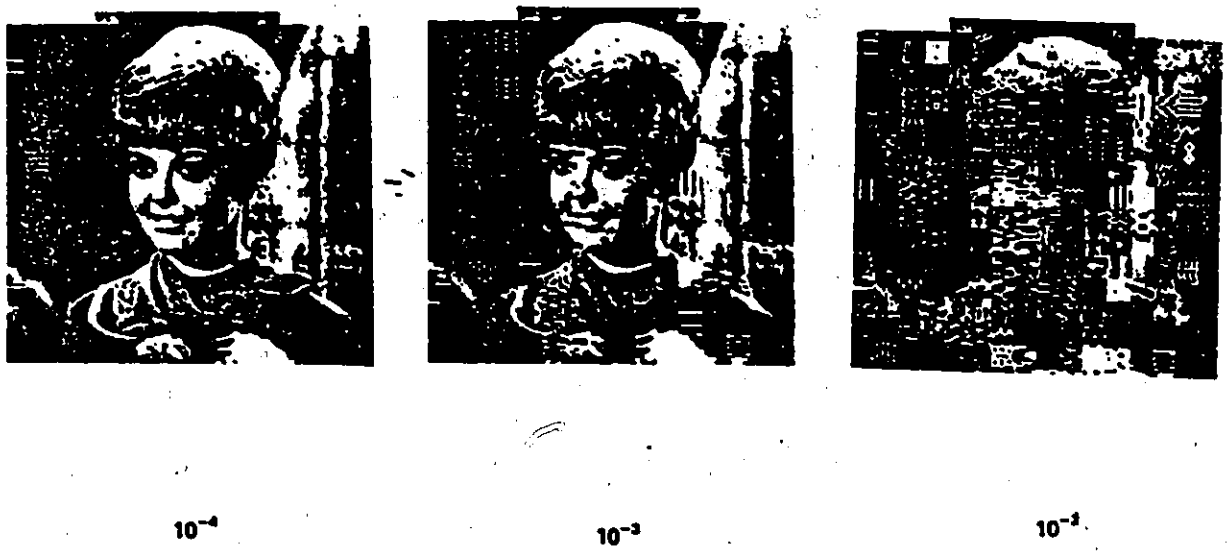

Figure 3.4: Channel error effects for slant transform coding in 16×16 pixel blocks at 1.5 bits per pixel for three bit error rates.

3.2 Error Protection Techniques for Intraframe Image Transmission

We note that as information is compressed into fewer bits, the effect of channel errors on reconstruction quality becomes more serious. Many error protection techniques have been developed, which can be basically classified as those with or without redundancy. In this thesis, these techniques are surveied by dividing into four categories:

1. Careful design and choice of source coding
2. Error detection using signal statistics, and error correction(smoothing).
3. Tandem combination of source-channel coding.
4. Joint source-channel coding.

3.2.1 Careful design and choice of source coding

There are ways of making coding systems inherently more robust to transmission errors. In other words, by careful designs of coder components such as transforms, quantizers and encoders it is possible to reduce the effects of channel error on image transmission.

For instance, Rydbeck and Sundberg showed [S1] that binary folded PCM code is less sensitive to digital errors than the standard binary folded PCM code for a large class of input signal density functions, e.g., exponential, Gaussian, etc. They also pointed out that there must be PCM codes even more insensitive to channel noise than binary folded PCM. By studying the input signal density function for low-input levels they observe that,

1. PCM words around the zero level are much more probable than the others,and
2. error sequences with single errors are the most probable ones.

Therefore, they presented a scheme, called MDC-PCM (minimum distance code), where the most probable PCM words have a small probability of single errors. That is, the code has the property that the errors are successively larger for less probable PCM words. In Table 3.1 [81] below we present a comparison among the different PCM codes: (1) binary folded PCM, (2) natural binary PCM and (3) MDC-PCM for low-input signal levels.

binary folded PCM	*natural binary PCM*	*MDC-PCM*
001111	010000	011000
001110	010001	010100
001101	010010	001100
001100	010011	010010
001011	010100	001010
001010	010101	000110
001001	010110	010001
001000	010111	001001
000111	011000	000101
000110	011001	000011
000101	011010	010000
000100	011011	001000
000011	011100	000100
000010	011101	000010
000001	011110	000001
000000	011111	000000
100000	100000	100000
100001	100001	100001
100010	100010	100010
100011	100011	100100
100100	100100	101000
.	.	.
.	.	.
.	.	.
111111	111111	111111

Table 3.1: MDC for 6-bit PCM. The first digit is a sign digit giving symmetry around the zero level. For the sake of comparison the 6-bit natural binary PCM and binary folded PCM codes are also shown.

3.2.2 Error detection using signal statistics, and error correction(smoothing)

In this section, we describe Difference Detection and Correction technique [83, 85, 87, 86, 95, 67], which achieve error protection by exploiting the redundancy inherent in most images. The error protection techniques can be realized at the receiver without recourse to any channel coding. In the other words, the systems really exist only at the receiver. In the difference detection and correction system [83], the detection procedure is based on the sample-to-sample differences in the received signal. It examines each sample in the decoded sequence q_k and for the ith component q_i considers it to be erroneous only if

$$|q_i - Q_{i-1}| > L\sigma_d \tag{3.2}$$

where Q_{i-1} is the corrected sample at the $(i-1)$th instant, or q_{i-1} sample if q_{i-1} was detected and considered to be correct. σ_d is the r.m.s. value of the differences between adjacent samples in a block of decoded samples, and L is a system parameter. On the detection of an error, the sample is replaced by the result of the correction procedure and subsequent samples are adjusted to compensate for the error propagation.

Various detection and correction methods have been developed for PCM, DPCM and TC. For instance, correlation measurements and sample-to-sample difference measurements for PCM were presented in [87], detector based on sample-to-sample difference measurements for DPCM was presented in [83, 86]. However, all the approaches mentioned above appear to be inadequate for the enhancement of badly corrupted pictures.

3.2.3 Tandem combination of source-channel coding

In this section, we introduce approaches that achieve error protection by the tandem combination of source and channel coding. The techniques require recourse of channel coding techniques.

Modestino and Daut [63] demonstrated that when an image is transmitted through noisy

channel, the resulting mean-square reconstruction error e_{ms}^2 can be expressed as the sum of the three individual components:

$$e_{ms}^2 = \epsilon_q + 2\epsilon_m + \epsilon_c \tag{3.3}$$

where ϵ_q represents the mean-square value of the quantization noise normalized on a pixel basis, ϵ_c represents the normalized mean-square error contribution solely due to channel errors, and ϵ_m represents a mutual error term due to the interaction of the quantization and channel errors. There is a tendency to assume that the quantization and the channel errors are independent and zero-mean and hence $\epsilon_m = 0$.

$$e_{ms}^2 = \epsilon_q + \epsilon_c \tag{3.4}$$

However, in general this is not the case. Therefore, the reconstruction error is the sum of contributions due to quantization noise and channel errors. Modestino and Daut also showed this conclusion through experiments. That is, the coding performance decreases rapidly in the presence of noise, and for a noisy channel the degradation in coding performance cannot be improved by simply increasing the source coding bit rate as it is discussed in section 3.1.2 and 3.1.3. Hence, they [64] presented a combined source-channel coding scheme for images which can lead to improvements in reconstructed image quality in the presence of channel errors while maintaining a fixed transmission bandwidth. This improvement is achieved by dividing the encoding rate between the quantization accuracy and channel coding. The three error protection schemes they presented are: protection to (1) to every bit of information (Protection 1), (2) to every bit of the most significant components of the information (Protection 2), and (3) to the most significant bits of the information (Protection 3).

A few extensions to Modestino and Daut's approach have been developed [20, 65, 99, 90]. Tanabe and Farvardin [90] have applied the combined source-channel coding concept to subband coding, where the percentage of bit rate dedicated to error protection increases for noisier channels.

3.2.4 Joint source-channel coding

In this section, we introduce approaches that achieve error protection by designing quantizers which take into account the channel noise but do not require recourse of channel coding techniques.

We note that the necessary condition for minimizing the mean distortion in scalar quantization was first presented by Lloyd and Max, and then the necessary conditions for minimizing the mean square error was obtained by Kurtenbach and Wintz [54] from a more generalized standpoint considering channel errors. They show the quantization values $v_l (l = 1, ..., m)$ and transition levels $u_k (k = 2, ..., m)$ which minimize the total mean-square error for any given input probability density $p_x(X)$ and any given channel matrix $P = \{P_{kl}\}$. The results are as follows,

$$v_j = \frac{\sum_{k=1}^{N} P_{kj} \int_{uk}^{uk+1} X p_x(X) dX}{\sum_{k=1}^{N} P_{kj} \int_{uk}^{uk+1} p_x(X) dX} \qquad j = 1, ..., N \tag{3.5}$$

$$u_j = \frac{1}{2} \frac{\sum_{l=1}^{N} v_l^2 (P_{jl} - P_{j-1,l})}{\sum_{l=1}^{N} v_l (P_{jl} - P_{j-1,l})} \qquad j = 1, ..., N \tag{3.6}$$

where N is the number of quantization levels.

We can see that the quantization values v_l and transition levels u_k depend on the probability density function $p_x(X)$ of input data, and the channel transition matrix $P = \{P_{kl}\}$. Hence, they are restricted to non-lookahead coding systems. This quantizer by Kurtenbach includes the quantizer by Lloyd and Max as a special case. They pointed out that only a slight improvement can be made by implementing a quantizer optimized for the noisy channel.

We note that Gray codes have the property that code words within a small Hamming distance from each other correspond to PCM amplitude levels which are close to one another. Hence, we can see that the average distortion in reproducing the analog signal in the presence of channel noise can be reduced by using a Gray code. Zeger and Gersho [100] extend this concept to the design of vector quantizers over noisy channels. We recall that in vector quantization the binary labels of optimally chosen codewords are transmitted as address for

the representative vectors (codewords). The decoding steps in vector quantization is a simple table look-up procedure. Thus, a distortion is introduced when the channel errors changes the transmitted binary labels. By designing the codebook in such a way that labels within a small Hamming distance from one another correspond to codewords within a small distance from one another, the average distortion caused by channel errors can be reduced.

In their algorithm [100], an initial codebook $W_0 = \{w'_0, w'_1, ..., w'_{N-1}\}$, whose labels $I = \{0, 1, ..., 2^b - 1\}$ correspond to an initial and perhaps arbitrary ordering of the codewords, is generated. Suppose an input vector v which is approximated (vector-quantized) by the codeword w_i, so that the label i is transmitted. However, possible channel errors may cause label j to be received. By minimizing the total distortion due to the combined effect of the quantization and channel index errors,

$$d(v, w_j) = d(v, w_i) + [d(v, w_j) - d(v, w_i)] \tag{3.7}$$

the rearrangement, a one-to-one mapping $f : I \rightarrow W_0$, of the initial codebook W_0 which uniquely assigns a codeword from W_0 to each label i in I can be achieved. Then a newly ordered codebook $W = \{w_0, w_1, ..., w_{N-1}\}$, whose codewords are $w_i = f(i)$, is generated.

3.3 Summary

A short review of error protection techniques for various intraframe coding schemes was presented. Four kinds of error protection methods are detailed in section 3.2. They are: (a) careful design and choice of source coding; (b) error detection exploring signal statistics, and error correction(smoothing); (c) tandem combination of source-channel coding; (d) joint source-channel coding for noisy channel. We note that the concept of tandem combination of source-channel coding is applied to the interframe coding in our research.

Chapter 4

Performance of Frame Replenishment Coding Techniques over Noiseless Channels

4.1 Introduction

We recall from chapter 2 that since Mounts proposed the basic frame replenishment coding (BFR), a number of modification to this algorithm have been proposed. Two frame replenishment coding techniques using vector quantization, namely, label replenishment vector quantization (LRVQ) and codeword replenishment vector quantization (CWRVQ) were presented by Goldberg and Sun. In this chapter, the coding performance over noiseless channels of BFR, LRVQ and CWRVQ is presented.

4.2 Performance of BFR, LRVQ and CWRVQ over Noiseless Channel

We note that coding performance is normally evaluated in terms distortion-rate criterion [75]. One of the commonly used measure as presented in section 2.2.2 is the signal-to-noise ratio (SNR_0) which is defined in :

$$SNR = 10 \log_{10} \frac{\sigma_s^2}{e_{ms}^2} (dB) \tag{4.1}$$

where σ_s^2 is the variance of the original image. A generalization to interframe image coding performance leads to the result:

$$SNR_0 = 10\log_{10}\frac{\sum_i \sum_j \sum_k s(i,j,k)^2}{\sum_i \sum_j \sum_k (s(i,j,k) - \hat{s}(i,j,k))^2} \tag{4.2}$$

where s and $\hat{s}$ are the original image array and the reconstructed estimate of s at the receiver, respectively.

We now turn to the computation of the bit rate. Table 4.1 shows the different component of information that needs to be transmitted for the three chosen frame replenishment techniques.

Coding Technique	*Side Information*	*Transmitted Updating Elements*
BFR	address of changed pixels	values of changed pixels
LRVQ	map of changed labels	values of changed labels
CWRVQ	map of changed labels	values of changed labels and codewords

Table 4.1: The transmitted information in BFR, LRVQ and CWRVQ

It can be seen that there are two components to the frame bit rate R^j for frame replenishment coding,

$$R^j = R_s^j + R_c^j \tag{4.3}$$

Here R_s^j is the side information to specify replenished elements and R_c^j is the bit rate required for updating changed elements. We note that the position of changed pixel in conditional frame replenishment coding [66] is indicated using the address of the updated pixel. We refer to this as the address method. An alternative approach [30] is the map method where 1 bit/per pixel is used to represent the position of changed information. Our simulations present results for both methods.

4.3 Simulation and Discussion of Results

In this thesis, computer simulations are carried out on two image sequences, one [see Fig. 4.1] is an extract of the CCETT image sequence of a woman talking on a telephone, consisting

of 20 frames of size 112×96 pixels and quantized to 8 bits/pixel. In this image sequence, the first 9 frames of the sequence are fairly constant; the next 5 frames exhibit a rapid motion of the face; and finally, the last 6 frames have relatively small changes. The second [see Fig. 4.2] is an angiogram image sequence of eight frames, 256 pixels by 256 pixels, with 8 bits of resolution, extracted from an angiographic X-ray sequence supplied by CGR of France. In this image sequence, a radio-opaque contrast dye is injected into the blood system with organ motion such as cardiac pulsation, breathing and swallowing. Our experiments are mainly performed on the first image sequence, the face image sequence.

To demonstrate the performance of frame replenishment coding techniques, three kinds of measures are used in this thesis:

1. overall signal-to-noise ratio.

2. the bit rate as a function of the frame number, and

3. the signal-to-noise ratio as a function of the frame number.

The first is on a global source basis and is used to compare the coding performance over the image sequences. The other two are on a local, frame-to-frame basis.

4.3.1 Simulation results

In the first set of experiments, the coding performance of BFR, LRVQ and CWRVQ over noiseless channel is evaluated and reproduced in Fig. 4.3 - Fig. 4.6. The performance of the three frame replenishment techniques with two different addressing schemes for the two image sequences graphed in Fig. 4.3 and Fig. 4.4 show that significant gains can be obtained by using LRVQ and CWRVQ techniques. We observe that better coding performance is obtained using BFR-add, LRVQ-map and CWRVQ-map respectively. Hence, further experiments on source coding techniques and combined source channel coding techniques over noisy channels have been performed on BFR-add, LRVQ-map and CWRVQ-map techniques. It can be seen from

Fig. 4.5 and Fig. 4.6 that BFR exhibits high sensitivity to motion in the picture in contrast to LRVQ and CWRVQ.

4.3.2 Discussion of results

The results of the first set of experiments demonstrate the superior coding performance of LRVQ and CWRVQ techniques in a noiseless channel.

Discussion of average coding performance

The comparison of the performances of the three frame replenishment techniques with two different addressing schemes for the face image sequence and the angiogram image sequence graphed in Fig. 4.3 and Fig. 4.4 demonstrates that in general LRVQ and CWRVQ are more efficient coding schemes than BFR. Also LRVQ and CWRVQ using the map method are better than using the address method.

Discussion of motion sensitivity

The curves on a frame-by-frame basis for the three schemes are shown in Fig. 4.5 and Fig. 4.6 respectively. The sensitivity to changes in the pictures (Fig. 4.5) shows that at a fixed SNR_0, BFR needs much more bits to provide the same performance as LRVQ and CWRVQ. We note that when the image sequence begins to become active at frame 9 and 10, the bit rate for BFR more than doubles and remains high for the rest of the sequence. As a result, BFR is much more sensitive to the motion in the sequence than LRVQ and CWRVQ. For a fixed average bit rate, it can be seen from Fig. 4.6 for the face image sequence that if the sequence is fairly constant, BFR outperforms LRVQ and CWRVQ. This results from the fact that in the regions where there is little motion, BFR using the address method requires only a few bits to indicate the changed information in contrast to the LRVQ and CWRVQ using the map method. We note that when the image becomes active, the SNR for the BFR technique

decreases substantially (by about 45%), but the SNR for LRVQ and CWRVQ are almost constant. Hence, BFR is very sensitive to changes in the image sequence.

For a fixed average bit rate 0.5(bit/pixel), signal-to-noise ratio as a function of frame number for BFR, LRVQ and CWRVQ applied to the angiogram image sequence is shown in Fig. 4.7. The results also show tolerance of LRVQ and CWRVQ for the arrival of contrast dye material in the arterial system after frame 5.

In summary, it can be observed from the results of the first set of experiments that LRVQ and CWRVQ provide more efficient coding than BFR, and are more tolerant to change in the pictures than BFR.

Pictorial results

The reconstructed images corresponding to Fig. 4.6 are provided in Fig. 4.8 for BFR and LRVQ. The transmission bandwidth requirements are kept constant for all the reconstructed images. These pictures illustrate the superior coding performance of LRVQ technique in a noiseless channel and the serious sensitivity to the changes in the images for BFR. For example, in Fig. 4.8, we see that when there is rapid motion in the sequence, the reconstructed images using BFR become quite poor. Compared with BFR, LRVQ is an efficient coding technique which can follow the rapid changes in the image sequence.

4.4 Summary

We have presented the coding performance of basic frame replenishment coding (BFR), label replenishment coding (LRVQ) and codeword replenishment coding (CWRVQ). Simulation results demonstrate the excellent coding performance and high tolerance to motion of LRVQ and CWRVQ.

Figure 4.1: Original Frame 7, 10, 13, and 17 from the original image sequence of a girl talking on the phone.

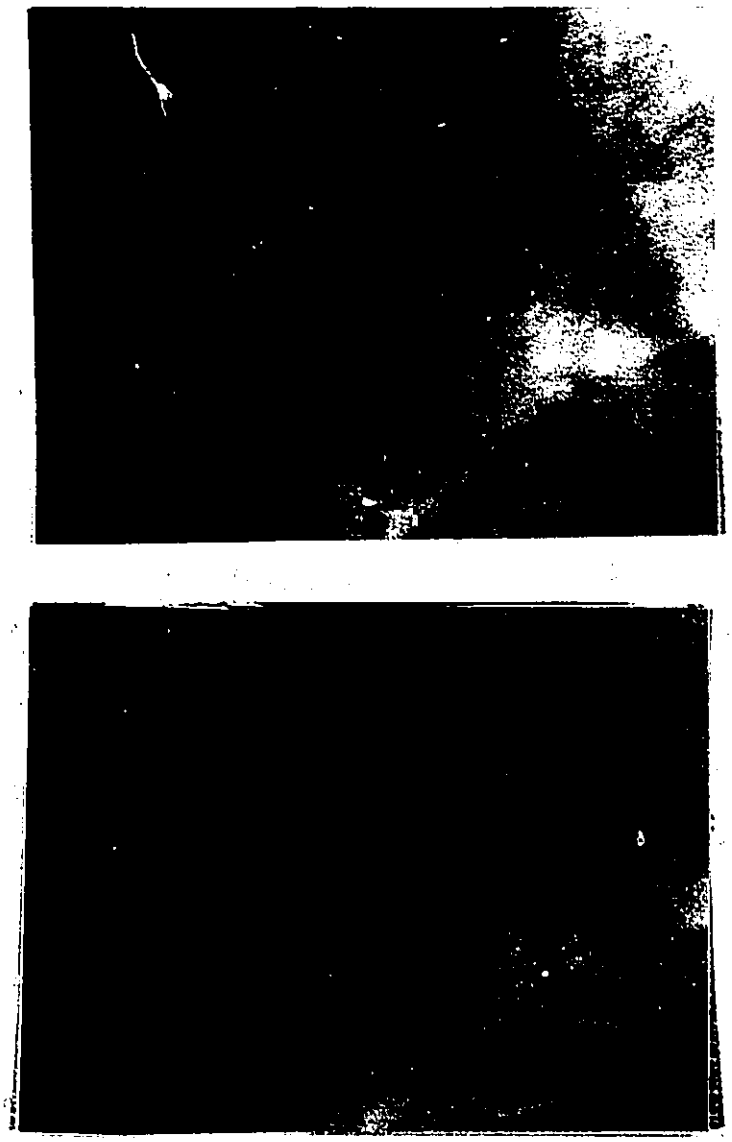

Figure 4.2: 112 × 96 pixel portions of the first frame (before the arrival of the contrast dye) and frame 6 (the presence of contrast dye in the arterial system) of angiogram image sequence.

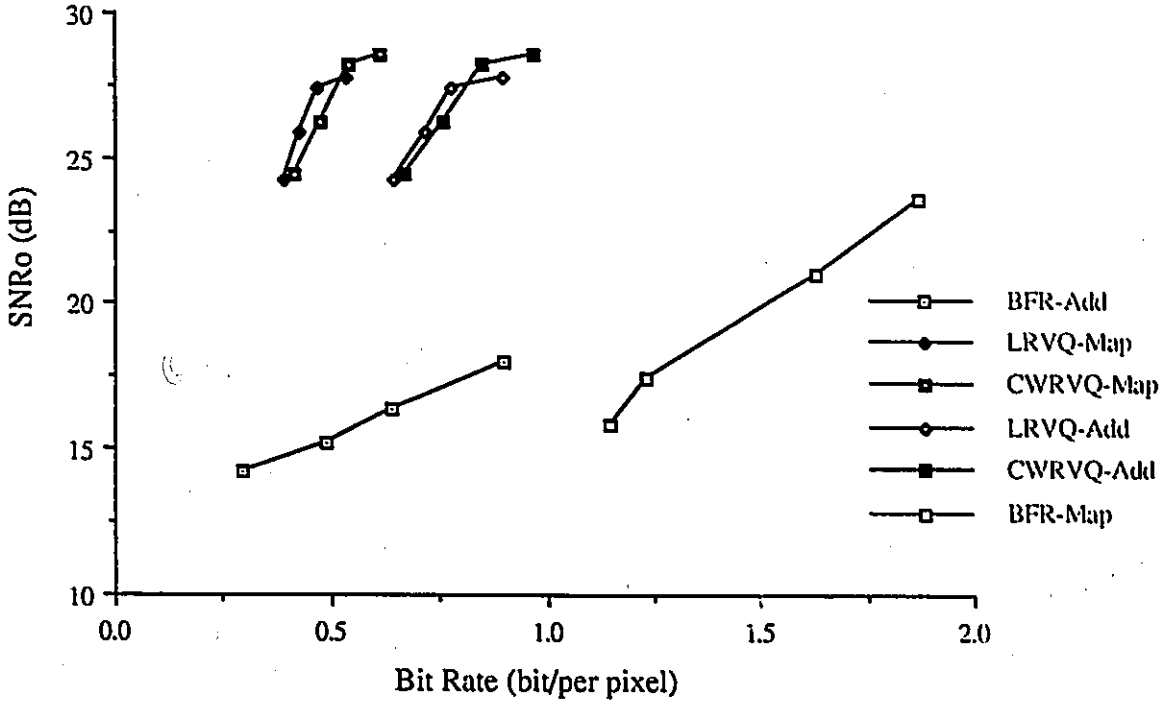

Figure 4.3: Comparison of six frame replenishment coding techniques for the face image sequence.

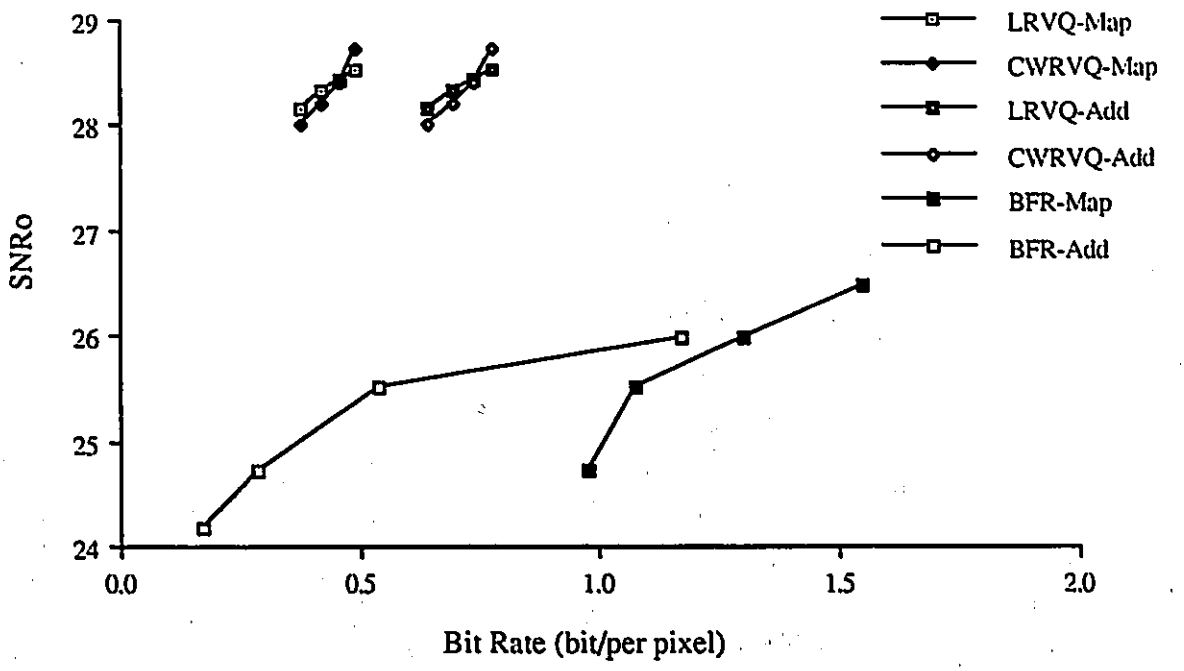

Figure 4.4: Comparison of six frame replenishment coding techniques for the angiogram image sequence.

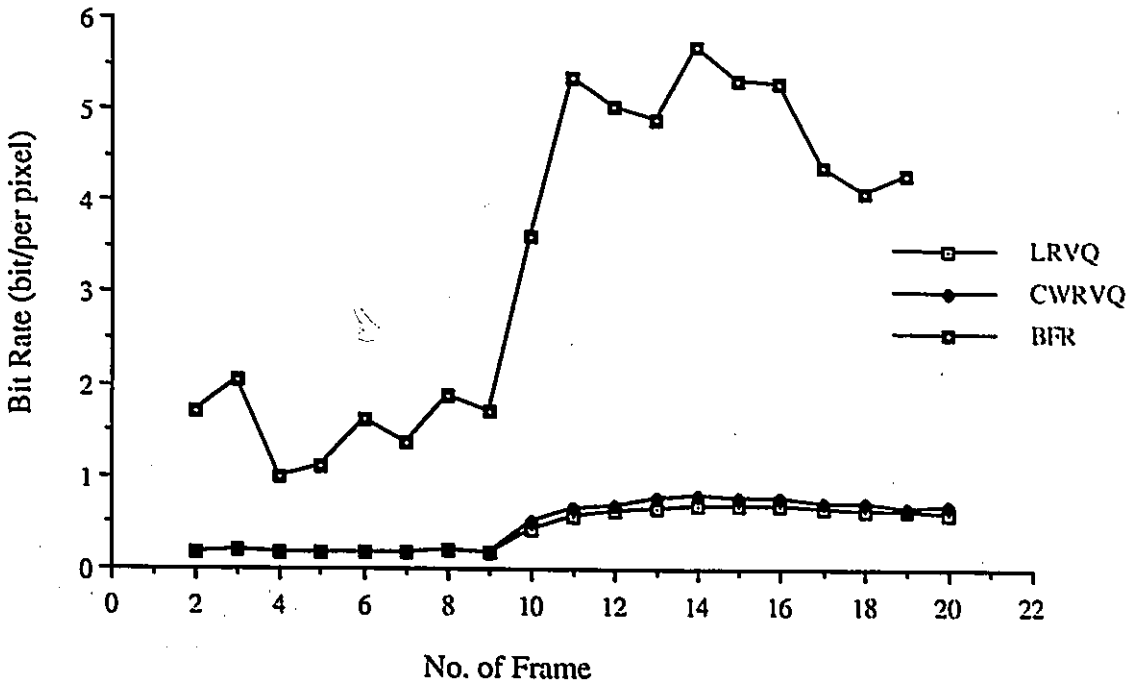

Figure 4.5: Bit rate as a function of number of frame for BFR, LRVQ and CWRVQ, at fixed $SNR_0 = 26dB$ for the face image sequence.

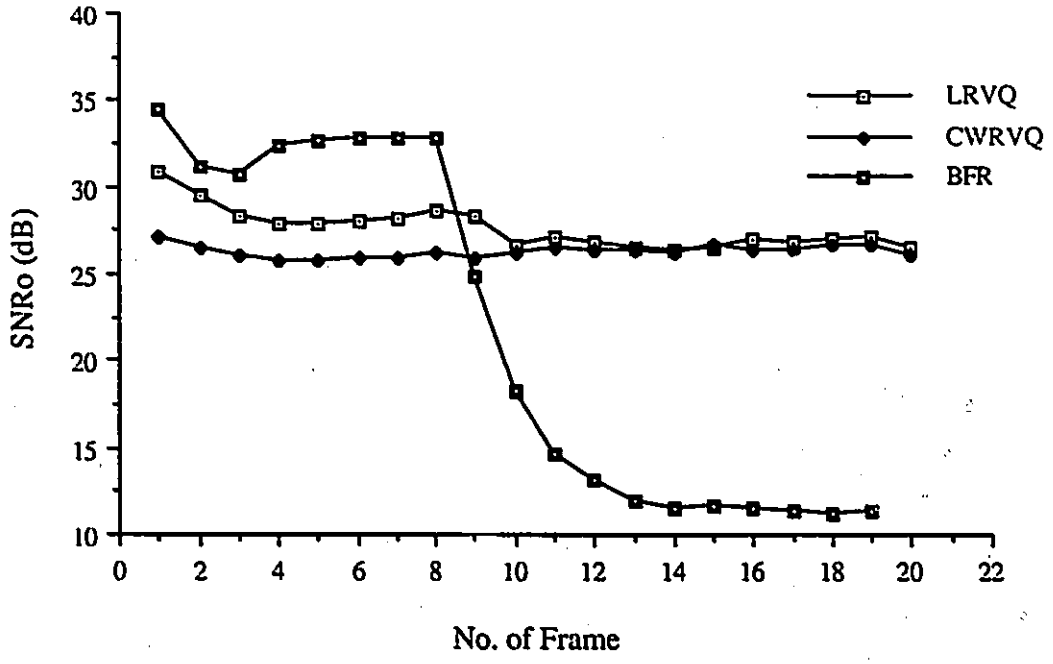

Figure 4.6: Signal-to-noise ratio as a function of frame number for BFR, LRVQ and CWRVQ applied to the face image sequence, at average bit rate =0.48($bit/pixel$).

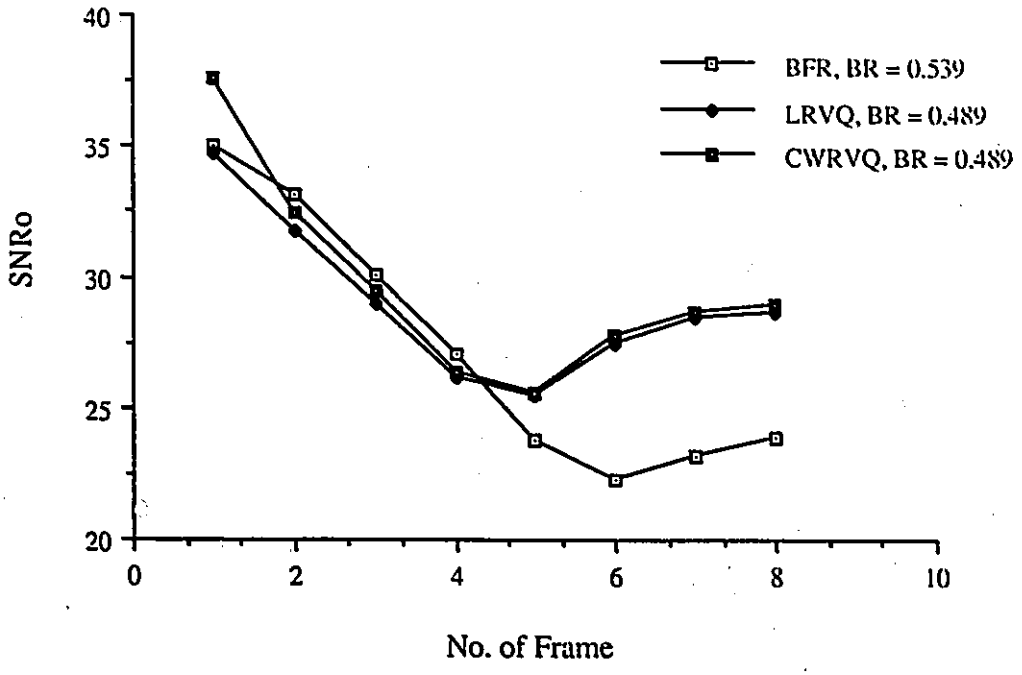

Figure 4.7: Signal-to-noise ratio as a function of frame number for BFR, LRVQ and CWRVQ applied to the angiogram image sequence, at average bit rate =0.5($bit/pixel$).

(a)

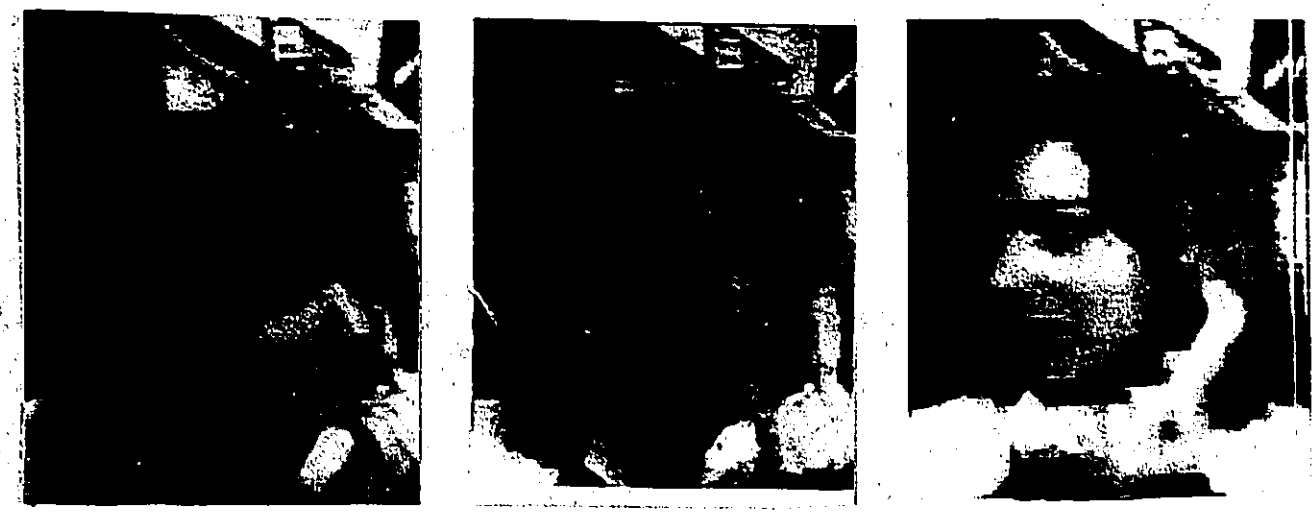

(b)

Figure 4.8: The pictorial results for the 7-th, 13-th and 17-th frames in (a) BFR with 0.49 bit/pixel and (b) LRVQ with 0.5 bit/pixel.

Chapter 5

Performances of Frame Replenishment Coding Techniques over Noisy Channels

5.1 Introduction

In this chapter, we present the performance of three frame replenishment coding techniques BFR, LRVQ and CWRVQ over noisy channels. We recall from chapter 2 that most of the source coding problems have been studied under the assumption that the communication channel is noiseless. But in practice channel errors occur and result in error in signal reconstruction. Therefore, we investigate the performance of the three frame replenishment coding, BFR, LRVQ and CWRVQ, over noisy channels. First an analysis of output signal-to-noise ratio for image transmission is detailed, and then the error propagation and average noise effect, for the three image sequence transmission techniques are studied.

5.2 Analysis of Output Signal-to-Noise Ratio

As mentioned in Eq. 2.5 and Eq. 4.2, the output signal-to-noise ratio (SNR_0) associated with coding an $M \times M \times K$ image block is given by

$$SNR_0 = \frac{\sigma_s^2}{e_{ms}^2} \tag{5.1}$$

where σ_s^2 is the variance of the assumed zero-mean stationary 3-D image data sequence $s(i,j,k)$ and

$$e_{ms}^2 = \frac{1}{M^2K} E\{\|s(i,j,k) - \hat{s}(i,j,k)\|^2\} \tag{5.2}$$

is the resulting mean-square reconstruction error. Here we make use of the norm $\| \ \|$ defined on the space of $M \times M \times K$ matrices according to

$$\|B\|^2 = trBB^* = \sum_{i=0}^{M-1} \sum_{j=0}^{M-1} \sum_{k=0}^{K-1} |b(i,j,k)|^2 \tag{5.3}$$

where, $s(i,j,k)$ is the original image array $M \times M \times K$, and $\hat{s}(i,j,k)$ is the reconstructed estimate of $s(i,j,k)$ at the receiver. The array $\hat{s}$ differs from s due to the quantization effects and the effects of channel noise. We model these effects as additive so that the estimate of the received image array $\hat{s}(i,j,k)$ is given by [63]

$$\hat{s}(i,j,k) = s(i,j,k) + q(i,j,k) + n(i,j,k) \tag{5.4}$$

Here, $q(i,j,k)$ represents the additive quantization noise associated with the (i,j,k) component and $n(i,j,k)$ represents the effects of channel errors. The corresponding arrays of quantization and channel noise elements are expressed as q and n, respectively.

It follows from Eq. 5.2 and 5.4 that $e_{ms}{}^2$ can be expressed as the sum of the three individual components

$$e_{ms}^2 = \varepsilon_q + 2\varepsilon_m + \varepsilon_c \tag{5.5}$$

Here,

$$\varepsilon_q = \frac{1}{M^2K} E\{\|q(i,j,k)\|^2\} = \frac{1}{M^2K} \sum_{i=0}^{M-1} \sum_{j=0}^{M-1} \sum_{k=0}^{K-1} E\{q^2(i,j,k)\} \tag{5.6}$$

represents the mean-square value of the quantization noise normalized on a pixel basis. Similarly,

$$\varepsilon_c = \frac{1}{M^2K} E\{\|n(i,j,k)\|^2\} = \frac{1}{M^2K} \sum_{i=0}^{M-1} \sum_{j=0}^{M-1} \sum_{k=0}^{K-1} E\{n^2(i,j,k)\} \tag{5.7}$$

represents the normalized mean-square error contribution solely due to channel errors. Finally,

$$\varepsilon_m = \frac{1}{M^2K} trE\{q(i,j,k)n^*(i,j,k)\} = \frac{1}{M^2K} \sum_{i=0}^{M-1} \sum_{j=0}^{M-1} \sum_{k=0}^{K-1} E\{q(i,j,k)n(i,j,k)\} \tag{5.8}$$

represents a mutual error term due to the interaction of the quantization and channel errors.

5.3 Performance of BFR, LRVQ and CWRVQ over Noisy Channels

In image sequence transmission, two kinds of noise effects must be considered: firstly, the channel noise introduced on a frame by frame basis and secondly the propagation effect of the noise introduced at a given frame. This second effect arises only when some interframe coding is used. We have expressed the coding performance over a noisy channel in terms of the SNR_0 (Eq. 4.2). It can be seen that the SNR_0 also includes a source coding noise effect ε_q. In order to evaluate the error propagation effect (due to channel error introduced at a given frame), we have to remove the effect of source coding noise ε_q and evaluate the error propagation effect in terms of the difference of the signal-to-noise ratio, $\triangle SNR_0$ defined by:

$$\triangle SNR_0 = SNR_0(without\ noise) - SNR_0(with\ noise) \tag{5.9}$$

5.3.1 Channel model

We recall from chapter 2 that the channel encoder transforms the information sequence into a discrete encoded sequence. Discrete symbols are not suitable for transmission over a channel. The *modulator* is used to transform each output symbol of the channel encoder into a waveform of duration T. A common modulator is binary-phase-shift-keyed (BPSK) modulation which generates one of two signals, $s_0(t)$ for an encoded "0" or $s_1(t)$ for an encoded "1",

$$s_0(t) = \sqrt{\frac{2E}{T}}\sin(2\pi f_0 t + \frac{\pi}{2}) \qquad 0 \le t \le T \tag{5.10}$$

$$s_1(t) = \sqrt{\frac{2E}{T}}\sin(2\pi f_0 t - \frac{\pi}{2}) \qquad 0 \le t \le T \tag{5.11}$$

where f_0 is a multiple of $1/T$ and E is the energy of each signal.

The common form of noise disturbance present in any communication system is *additive white Gaussian noise (AWGN)*. If the transmitted signal is $s(t)$, the received signal is

$$r(t) = s(t) + n(t) \tag{5.12}$$

where $n(t)$ is a Gaussian random process with one-sided *power spectral density (PSD)* N_0.

A simple and important channel model is called the *binary symmetric channel(BSC)* in which (1) binary modulation is used, (2) the amplitude distribution of the noise is symmetric, and (3) the demodulator output is quantized to 2 levels. When BPSK modulation is used on an AWGN channel with optimum coherent detection and binary output quantization, the BSC transition probability is just the BSPK bit error probability P_b given by,

$$P_b = Q(\sqrt{\frac{2E_b}{N_0}}) \tag{5.13}$$

where

$$Q(x) = \frac{1}{\sqrt{2\pi}} \int_x^\infty e^{-y^2/2} dy \tag{5.14}$$

$$SNR_i = \frac{E_b}{N_0} \tag{5.15}$$

and E_b is the signal energy per transmitted binary channel symbol, also $N_0/2$ is the double-sided noise spectral density in W/Hz; $Q(.)$ is the *complementary error function* of Gaussian statistics, and SNR_i is channel signal (bit) -to-noise ratio.

In this thesis, we choose coherent binary phase-shift keyed (BPSK) modulation over an additive white Gaussian noise (AWGN) channel and use channel SNR_i to be the measure of channel error. The relation between bit error probability P_b and channel signal-to-noise ratio SNR_i for BPSK [78] is shown in Tab. 5.1.

5.4 Simulation and Discussion of results

We have performed simulations by using BFR, LRVQ and CWRVQ for the noisy channel case.

5.4.1 Simulation results

The results for the second set of experiments on error propagation and noise effect are graphed in Fig. 5.1 - Fig. 5.7. We note that the error propagation of LRVQ and CWRVQ techniques

Channel SNR_i	*Bit error probability* P_b
10dB	3.87×10^{-6}
9dB	3.36×10^{-5}
8dB	1.91×10^{-4}
7dB	7.73×10^{-4}
6dB	2.39×10^{-3}
5dB	5.95×10^{-3}
4dB	1.25×10^{-2}
3dB	2.29×10^{-2}
2dB	3.75×10^{-2}
1dB	5.63×10^{-2}
0dB	7.86×10^{-2}

Table 5.1: Relation of channel SNR_i and bit error probability P_b (BPSK)

is much serious than BFR. We also note that the coding performance of BFR, LRVQ and CWRVQ decreases rapidly when the image sequence is transmitted over a noisy channel.

5.4.2 Discussion of results

The results of the second set of experiments clearly demonstrate deteriorating performance of LRVQ and CWRVQ in a noisy channel.

Discussion of error propagation

Simulations to study the effects of error propagation in BFR and LRVQ are performed for both the image sequence with little changes consisting of the first 10 frames of the face image sequence, and the image sequence with rapid changes consisting of the last 10 frames of the face image sequence introduced in the chapter 4. The results are shown in Fig. 5.1- Fig. 5.4. We recall from section 5.2 that ΔSNR_0 is used to evaluate the error propagation of each coding technique instead of SNR_0. This is due to the effect of source coding being removed from SNR_0. It can be seen clearly from Fig. 5.1-Fig. 5.2 that the error propagation of LRVQ and CWRVQ is much more serious than that using BFR both for the image sequence with

little changes and rapid changes. We note that the more one removes redundancy from an image sequence through the use of sophisticated coding techniques, the more important each bit of transmitted information becomes, and hence, the more noticeable are the effects of digital transmission errors [75]. It can be observed that for the LRVQ technique applied for the case of the image sequence with relatively small changes, the error propagation effects for channel errors introduced in the second frame continue to be persent in subsequent frames (at least until frame 10 when the image begins to be active), however, for the case of the image sequence with rapid motion of face, the error propagation effects reduce significantly in subsequent frames. This is due to the fact that when the image is rather still, the LRVQ technique requires few bits to indicate the changed information. Hence, most of the errors introduced in the second frame cannot be recovered by using the little replenished information from the subsequent frames. However, in the case of the image becoming active, the LRVQ technique requires much more bits to indicate the changed information in contrast to the case when there is little motion in the images. Hence, errors introduced in the second frame can be recovered by using the information from the subsequent frames. In Fig. 5.3-Fig. 5.4, we compare the coding performances of BFR and LRVQ with and without channel errors. It can be seen that even through BFR does not have serious error propagation effects, its performance is still 15 dB lower than LRVQ for the image sequence with rapid motion. The effect also can be seen from the pictorial results [see Fig. 5.8].

Discussion of noise effects

The noise effects of BFR, LRVQ and CWRVQ over 20 frames of the face image sequence are evaluated in term of SNR_0 and are compared in Fig. 5.5 - Fig. 5.7. It can be seen that LRVQ and CWRVQ are highly sensitive to channel errors, much more so than BFR. For example, at SNR_i = 8 dB, the coding performance of LRVQ decreases by 13 dB and CWRVQ by 14 dB, compared to 1 dB using BFR. It can also be seen that for channel SNR_i in excess of approximately 10 dB, channel errors are rare and the performance is limited solely by the source coding accuracy. Any increase in the bit rate results in an increase in SNR_0. However,

we see that the coding performance cannot be improved by increasing the source coding bit rate when SNR_i is lower than 8dB for LRVQ and CWRVQ , and 5dB for BFR. This is due to the fact that more transmitted bits are affected by noise when the coding bit rate is increased. It is proved that for each coding technique there is a SNR_io, when SNR_i higher than SNR_io the reconstruction performance can be improved by increasing the source coding bit rate; otherwise, a combined source-channel coding should be employed in order to achieve high-quality image sequence reconstruction. It can be observed that SNR_io is about 8dB for LRVQ and CWRVQ, 5dB for BFR.

Pictorial results

The reconstructed images corresponding to Fig. 5.2 and Fig. 5.6 are provided in Fig. 5.8 and Fig. 5.9 respectively. These pictures illustrate the two different error propagation effects and noise effects for LRVQ. For example, in Fig. 5.8, we see that the error propagation effects of LRVQ last a long time in the images with little changes, and that LRVQ has fast error recovery in the image sequence with rapid changes. In Fig. 5.9, we see the extent of the serious noise effects in LRVQ when the channel $SNR_i = 9dB$.

5.5 Summary

We have presented the performance of three frame replenishment coding techniques over noisy channels. Our simulation results show that more efficient coder, such as LRVQ and CWRVQ, result in more serious error propagation and noise effects. They are more sensitive to channel noise, and their coding performance decreases more rapidly than BFR. This points to the need for providing error protection which improve the performance of image transmission over noisy channel when the bandwidth is fixed. This is the objective of the next chapter.

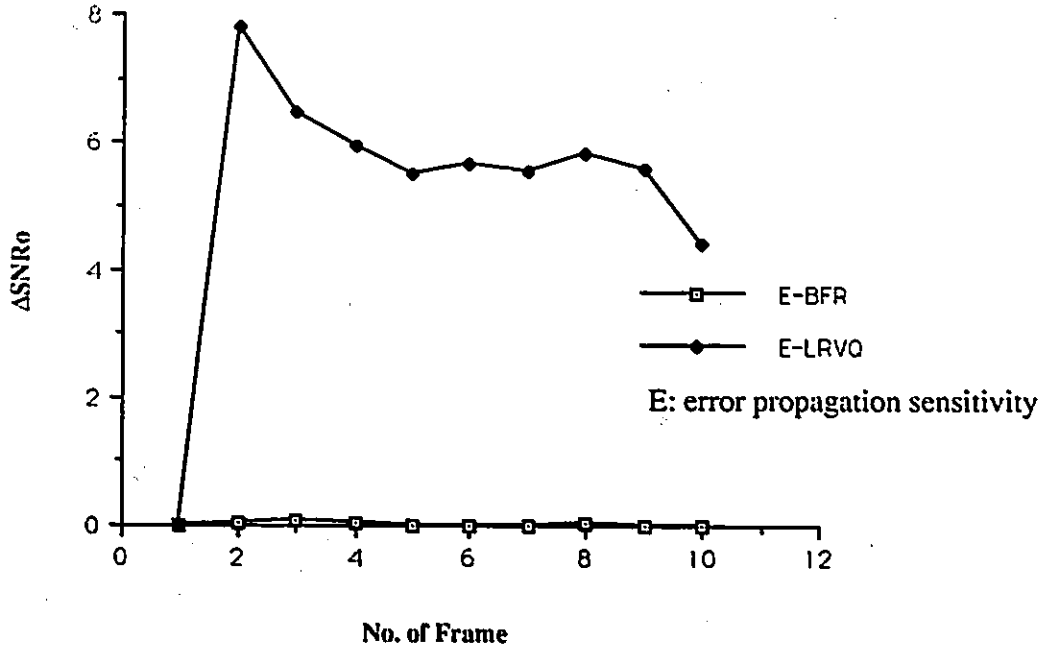

Figure 5.1: Error-propagation sensitivity of BFR and LRVQ for the face image sequence with little changes, channel $SNR_i = 8dB$.

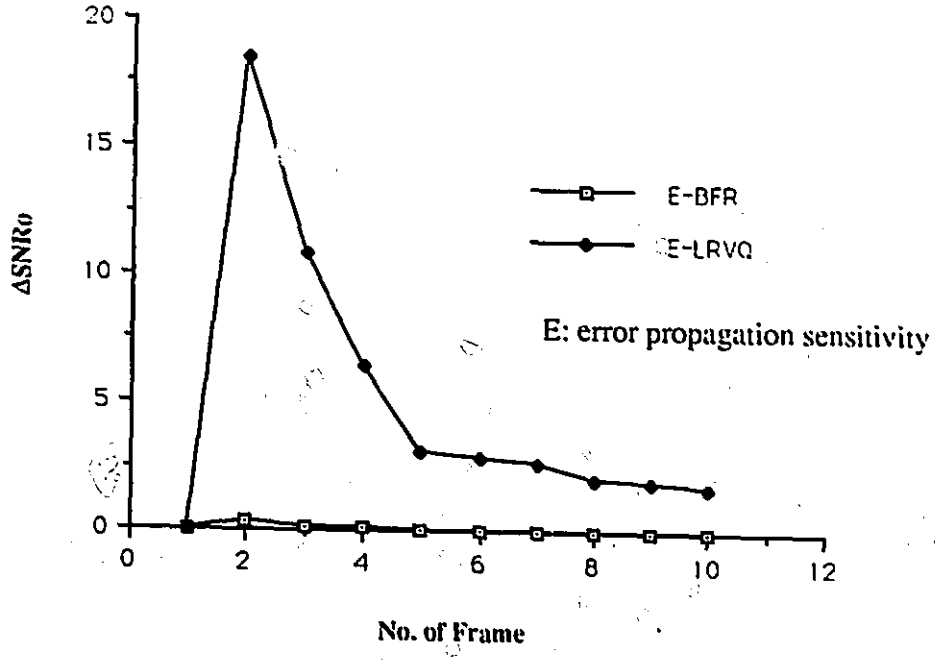

Figure 5.2: Error propagation sensitivity of BFR and LRVQ for the face image sequence with rapid changes, channel $SNR_i = 8dB$.

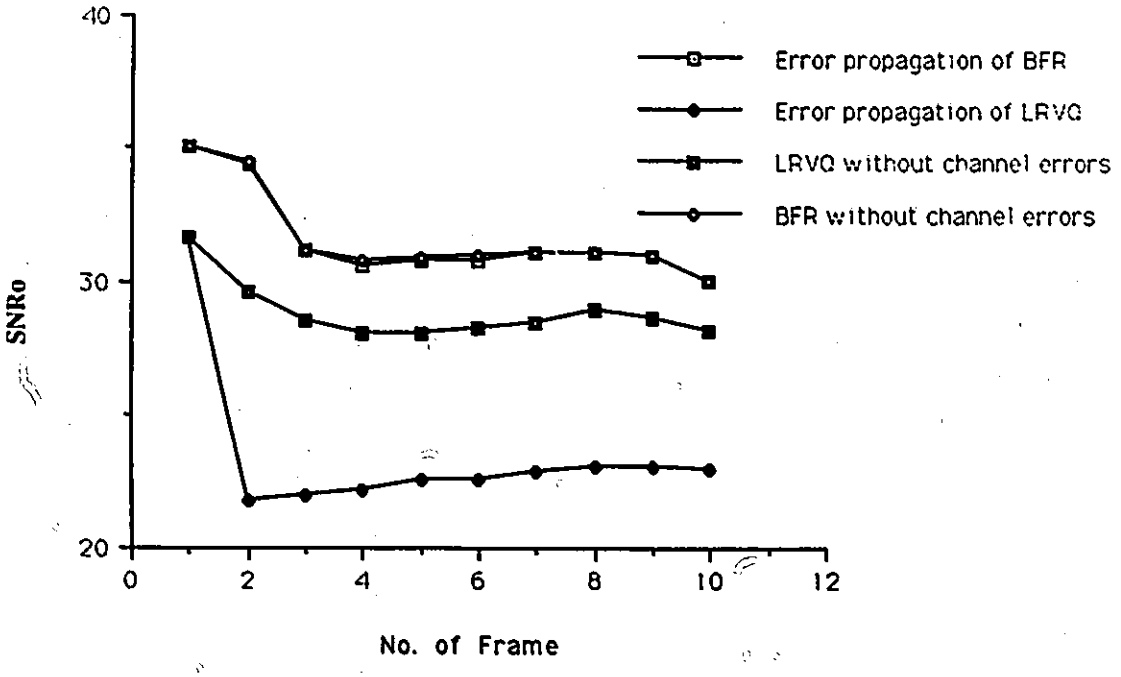

Figure 5.3: Error propagation for BFR and LRVQ over a $SNR_i = 8dB$ channel for face the image sequence with little changes.

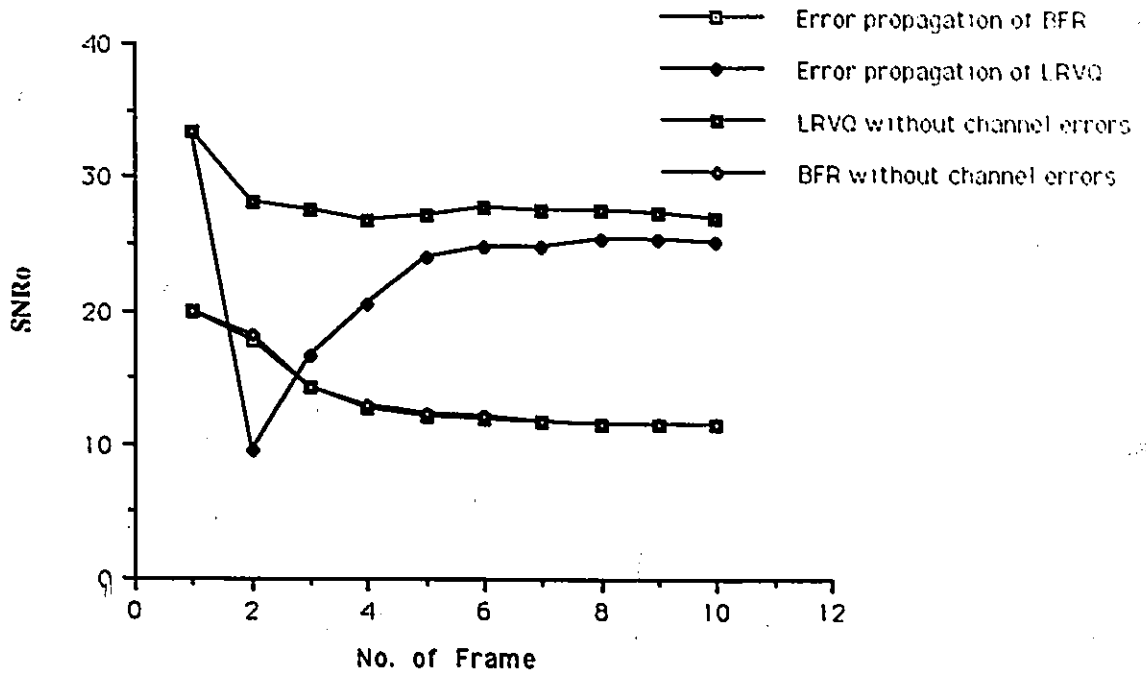

Figure 5.4: Error propagation for BFR and LRVQ over $SNR_i = 8dB$ channel for the face image sequence with rapid changes.

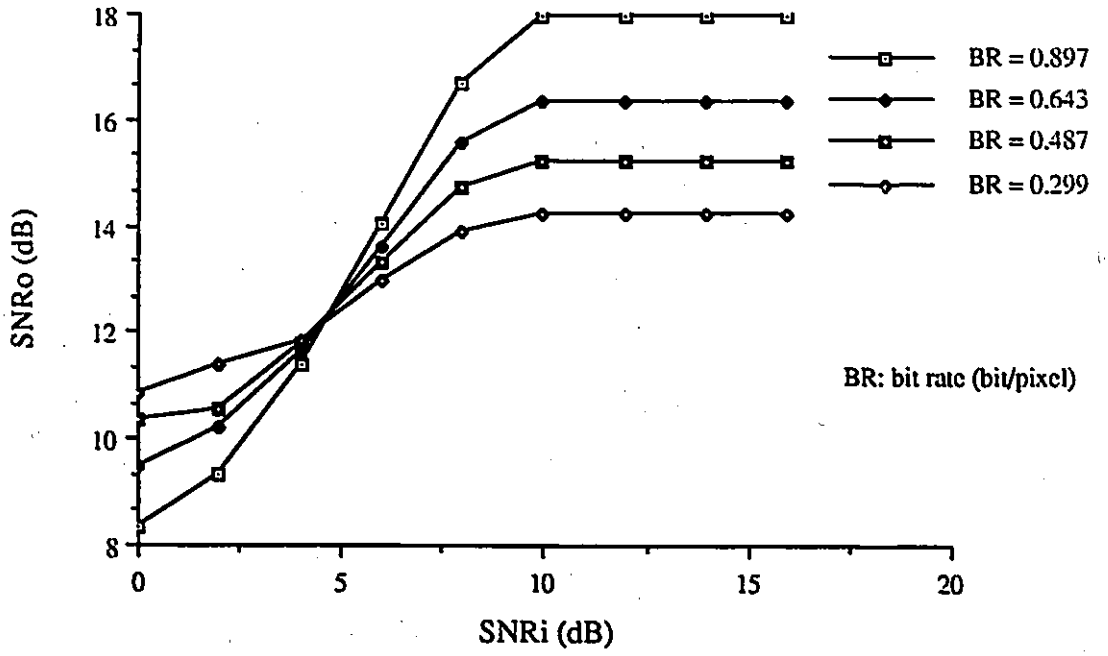

Figure 5.5: Coding performance of BFR with different bit rates as a function of channel noise.

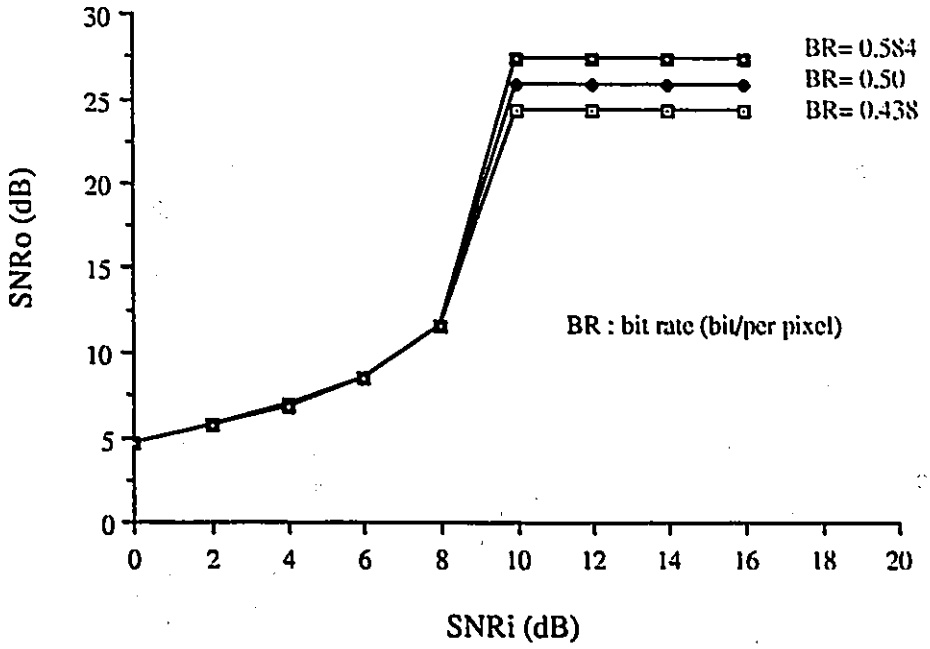

Figure 5.6: Coding performance of LRVQ with different codebook sizes as a function of channel noise.

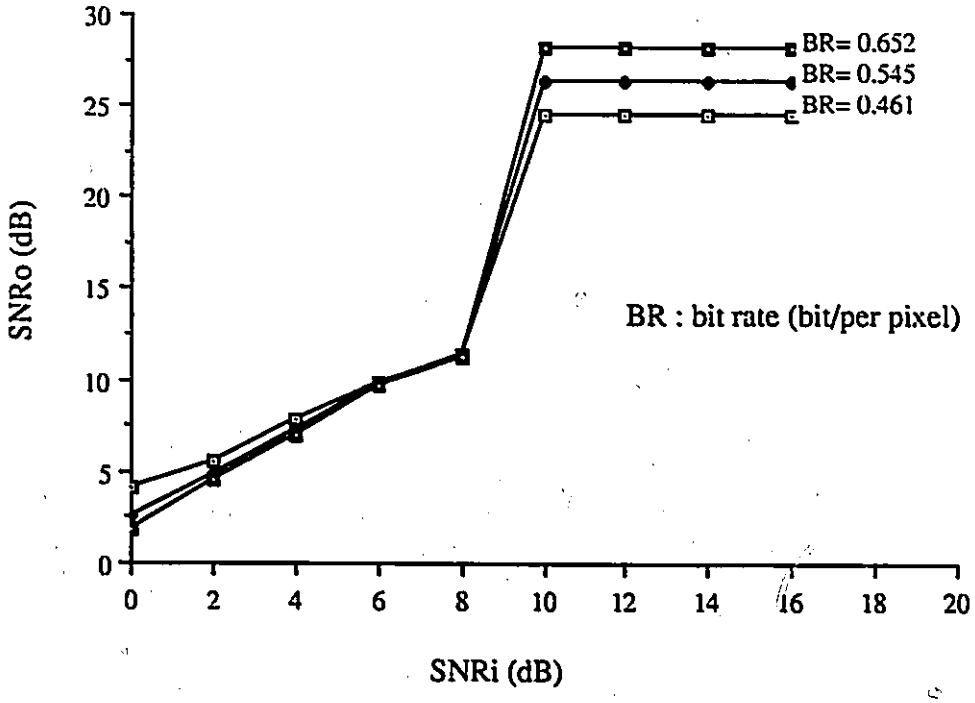

Figure 5.7: Coding performance of CWRVQ with different codebook sizes as a function of channel noise.

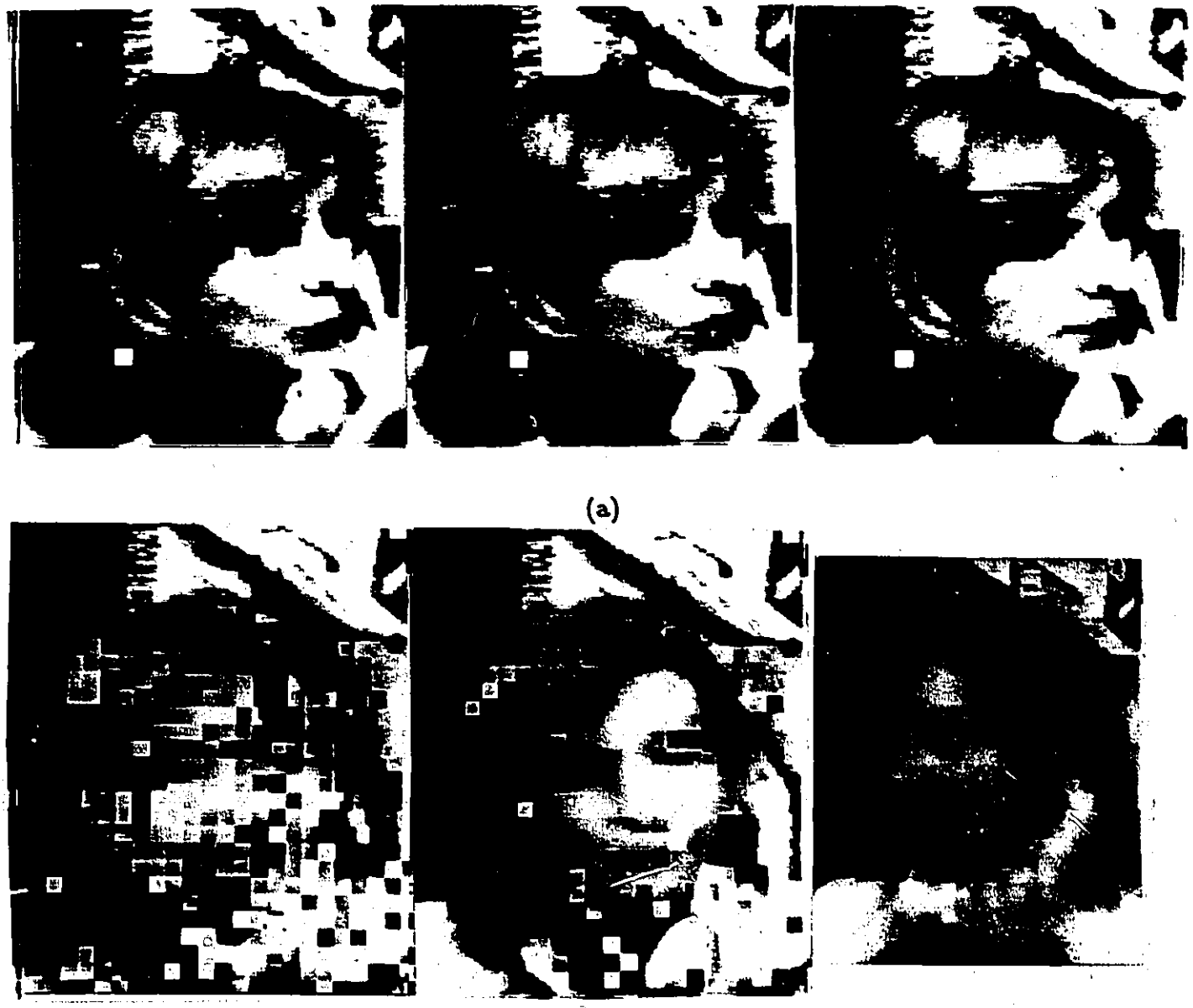

Figure 5.8: The pictorial results for the second, third and 7-th frames showing the error propagation in LRVQ over a channel $SNR_i = 8dB$. (a) Image sequence with little changes and (b) image sequence with rapid changes.

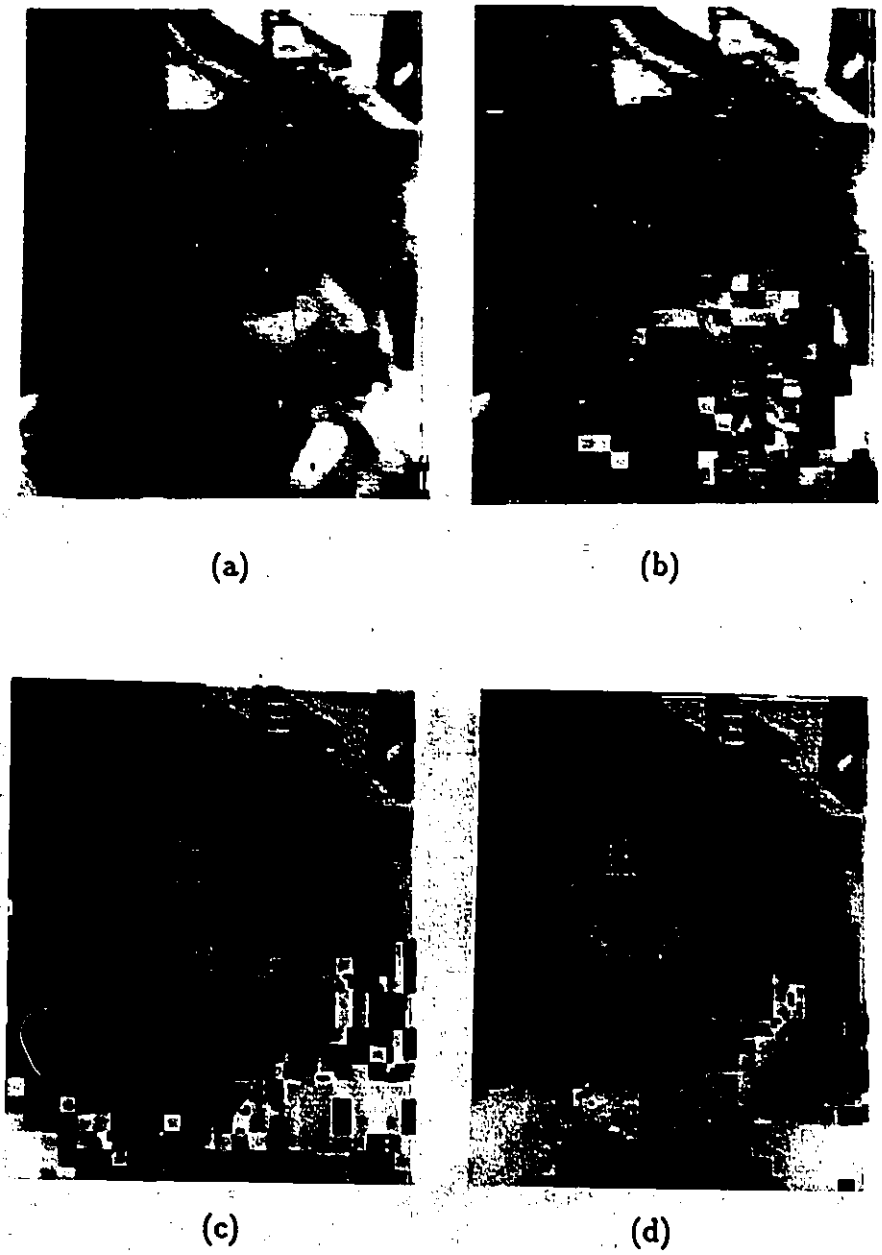

Figure 5.9: The pictorial results for the noise effects using LRVQ over a channel with SNR_i=9 dB channel: (a) the 8-th frame, (b) the 10-th frame, (c) the 15-th frame and (d) the 20-th frame.

Chapter 6

Performance of Combined Source-Channel Frame Replenishment Coding

6.1 Introduction

In the data compression designs considered in the previous chapters we ignored the channel effects by assuming noiseless channels. In practice, one of the most important problems in conventional image or voice communication systems where the information source and the receiver are connected with a communication channel is to minimize the distortion between the output signal of the information source and the receiving signal of the receiver under the condition that the number of bits transmitted through the channel is constant. Our simulation results in chapter 5 show that in the presence of channel errors, the behavior of LRVQ and CWRVQ degrades rapidly, and it is clear that we cannot provide higher source coding bit rate to improve the coding performance in noisy channel. As a result, some form of error control protection must be provided if high-quality image sequence reconstruction is to be achieved.

In chapter 3 four kinds of error protection methods for intraframe coding have been presented. In this chapter we extend the tandem combination of source-channel coding described in [63] to frame replenishment coding techniques with mean-square error as the performance criterion and present the performance of combined source-channel frame replenishment coding

techniques.

6.2 Combined Source-Channel Frame Replenishment Coding

It is known that to account for channel errors, one has to add redundancy to the input. On the other hand, data compression techniques tend to remove the redundancy in the source data. Thus a proper bit rate distribution between source coding (redundancy removal) and channel coding (redundancy injection) has to be achieved in the design of data compression systems. Since channel coding generally entails a bandwidth expansion, this operation can be extremely wasteful of channel bandwidth unless applied judiciously. In particular, bit rate distribution must be made between the reconstruction accuracy associated with the source coding and the degree of error control protection provided by the channel coding. Modestino [63], [64] presented a combined source-channel coding of images with three error protection schemes for intraframe differential PCM and intraframe transform coding which can provide good reconstructed image quality in the presence of channel errors, while maintaining a fixed transmission bandwidth. This improvement is achieved by trading quantization accuracy for error protection through channel coding. The Odenwalder [73] and Larsen [55] convolutional codes are used as error protection codes in the combined source channel transform coding. The three error protection schemes which have been considered in their paper are protections, (1) to every bit of information (Protection 1), (2) to every bit of the most significant components of the information (Protection 2), and (3) to the most significant bits of the information (Protection 3).

We apply the combined source-channel coding with the three error protection schemes similar to that of [64] to BFR, LRVQ and CWRVQ and compare the coding performance.

6.2.1 Channel coding

Channel codes may be divided into two main classes, *block codes* and *convolutional codes*. Convolutional codes are powerful error-correcting codes with relatively simple encoding and decoding schemes and have found application in many communication systems [78].

The encoder for a convolutional code accepts k-bit blocks of the information sequence u and produces an encoded sequence v of n-symbol blocks. (In convolutional coding, the symbols u and v are used to denote sequences of blocks rather than a single block.) Each encoded block depends not only on the corresponding k-bit message block at same time unit, but also on m previous message blocks. Hence, the encoder has a *memory order* of m. The set of encoded sequences produced by a k-input, n-output encoder of memory order m is called an (n, k, m) *convolutional code*. The ratio $R = k/n$ is called the *code rate*. For most of the useful convolutional codes the ratio $R = k/n$ are often $\frac{1}{2}, \frac{1}{3}, \frac{1}{4}, \frac{1}{5}, ...$, or $\frac{1}{2}, \frac{2}{3}, \frac{3}{4}, \frac{4}{5}, ...$

The *Viterbi algorithm* is a maximum likelihood (minimum distance) decision scheme for the decoding of the convolutional codes.

The Odenwalder convolutional code which has six delay elements (m=6) is drawn in the Fig. 6.1. It has 1 input, 2 outputs (R=1/2), and the generator polynomials are:

$$g^{(1)} = 1011011 \qquad (or\ 554\ in\ octal\ form) \qquad (6.1)$$

$$g^{(2)} = 1111001 \qquad (or\ 744\ in\ octal\ form) \qquad (6.2)$$

The Odenwalder convolutional code [73] is chosen as the error protection code in the thesis.

6.2.2 Schemes of error protection

The most significant transmitted information for Protection 2 and the most significant bit for Protection 3 have to be decided when the three protection schemes are applied to BFR,

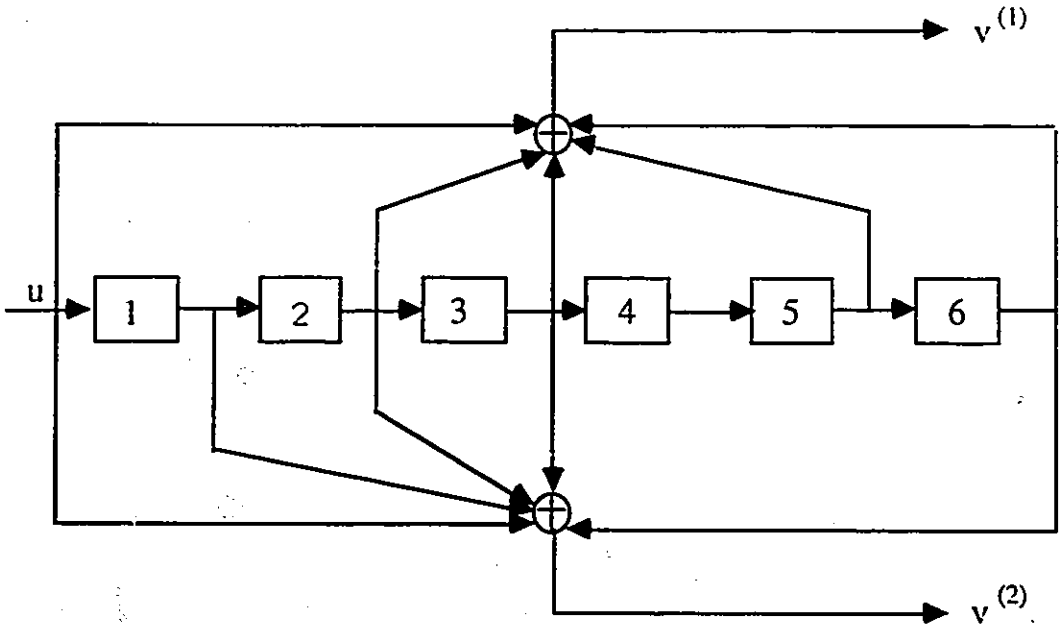

Figure 6.1: The (2,1,6) Odenwalder convolutional encoder.

LRVQ and CWRVQ. In our combined source-channel coding experiments, the side information to specify the changed elements is chosen as the most significant transmitted information for Protection 2, and the highest order bit of each transmitted information in the three techniques is chosen as the most significant bit for Protection 3. The protected elements chosen for the three Protections in BFR, LRVQ and CWRVQ are detailed in Table 6.1. Protection 0 is used to represent source coding without any error protections.

We can see from Table 6.1 that the percentage of bit rate allocation for error protection in Protection 1 is always fixed at 50% when the Odenwalder convolutional code ($R = 1/2$) is used for error protection. However, the percentages for Protection 2 and 3 differ for each technique because they depend on the particular transmission information selected.

Combined Source Channel Coding	*Protection* 1	*Protection* 2	*Protection* 3
BFR	address and value of changed pixels	address of changed pixels	highest order bit of address and value of changed pixels
LRVQ	map and value of changed labels	map of changed labels	highest order bit of map and value of changed labels
CWRVQ	map and value of changed labels, changed codewords	map of changed labels	highest order bit of map and value of changed labels, changed codewords

Table 6.1: The protected elements chosen for the three protections in BFR, LRVQ and CWRVQ

6.3 Simulation and Discussion of Results

6.3.1 Simulation results

The experimental results of combined source-channel coding are graphed in Fig. 6.2 - Fig. 6.5. It can be seen that for a fixed transmission bit rate, significant gains can be realized in noisy channels by using the combined source-channel coding.

6.3.2 Discussion of results

The results of combined source-channel coding performance for BFR, LRVQ and CWRVQ over the face image sequence are graphed in Fig. 6.2 - Fig. 6.4. The performance curves show the significant gains that can be realized with combined source channel coding using vector quantization (LRVQ and CWRVQ) for noisy channels by trading source coding accuracy for error protection. For example, from $SNR_i = 9dB$ to $SNR_i = 4dB$, combined source channel coding using LRVQ outperforms Protection 0 (LRVQ) in the range of $12dB$ to $2.5dB$, however, combined source channel coding using BFR outperforms Protection 0 (BFR) in the range of $1.5dB$ to $0dB$. The percentage of error protection is in the range of 22% - 50% of the total bit

rate in our experiments. However, for SNR_i in excess of approximately $10dB$, channel errors are rare and hence, the SNR_0 for the three error protection techniques are lower than SNR_0 for unprotected source coding.

Further comparisons of combined source channel coding schemes for BFR and LRVQ at a channel $SNR_i = 8dB$ are shown in Table 6.2, The results show that at $SNR_i = 8dB$,

Coding	*Protection*	*Total Bit Rate*	*Channel Bit Rate (%)*	$SNR_0(dB)$
BFR	0	0.642	0.000 (0%)	15.6
	1	0.588	0.294 (50%)	14.1
	2	0.619	0.148 (24%)	14.8
	3	0.627	0.188 (30%)	15
LRVQ	0	0.61	0.000 (0%)	11.49
	1	0.626	0.313 (50%)	20.3
	2	0.615	0.135 (22%)	21.9
	3	0.62	0.174 (28%)	23.3

Table 6.2: The comparison of combined source channel coding schemes for BFR and LRVQ at a channel $SNR_i = 8dB$.

Protection 3 (with 28% of bit rate used for error protection) for LRVQ provides the best performance; however, for BFR Protection 0 (with 0% of bit rate used for error protection) provides the best performance. This is due to the results we presented in chapter 5 that LRVQ and CWRVQ exhibit high sensitivities to channel errors, resulting in poor performance. Hence, for a fixed channel SNR_i the percentage of bit rate allocated to error protection in combined source channel coding schemes should be larger for more efficient coding, such as LRVQ and CWRVQ, to achieve the best performance.

The results of combined source channel coding performance for LRVQ over 20 frames are also summarized in Tab. 6.3, The results in Table 6.3 present that at $SNR_i = 8dB$, option 3 (28% error protection) has to be used to achieve the greatest improvement; however, at $SNR_i = 6dB$, option 1 (50% error protection) has to be used to achieve the greatest improvement. Hence, for a coding technique the percentage of bit rate allocated to error protection should be larger for a noisier channel.

SNR_i	*Protection*	*Total Bit Rate*	*Channel Bit Rate (%)*	$SNR_0(dB)$
6 dB	0	0.61	0.000 (0%)	8.48
	1	0.626	0.313 (50%)	17.5
	2	0.615	0.135 (22%)	14.5
	3	0.62	0.174 (28%)	16.6
8 dB	0	0.61	0.000 (0%)	11.49
	1	0.626	0.313 (50%)	20.3
	2	0.615	0.135 (22%)	21.9
	3	0.62	0.174 (28%)	23.3

Table 6.3: Performance of combined source-channel coding using label replenishment at design rates of 0.62 bpp.

The combined source channel coding schemes using LRVQ are also simulated for the angiogram image sequence shown in Fig. 6.5. It can be observed that the performance curves are similar as that for the face image sequence in Fig. 6.3. However, since the performance of Protection 0 (without any error protection) for the angiogram image sequence does not decrease as fast as that for the face image sequence in the Fig. 6.3 which is more active than the angiogram image sequence, there is less improvement in coding performance when combined source channel coding schemes to the angiogram image sequence.

Pictorial results

The reconstructed images corresponding to Fig. 6.3 are provided in Fig. 6.6 for LRVQ. The transmission bandwidth requirements are kept constant for all reconstructed images. These pictures illustrate the improvements in subjective quality of reconstructed image resulting from tradeoffs between source coding accuracy and error-control protection in a fixed transmission bandwidth. For example, in Fig. 6.6, we see the advantages in allocating excess transmission bandwidth to channel error control rather than in attempting to improve the reconstructed images by increasing the average number of bits/pixel used exclusively for source coding.

6.4 Summary

We have presented the performance of combined source channel coding techniques with three error protections. Our simulation results show that combined source channel coding provides significant improvement in coding performance over noisy channels without sacrificing bandwidth, especially for efficient coding techniques, such as LRVQ and CWRVQ.

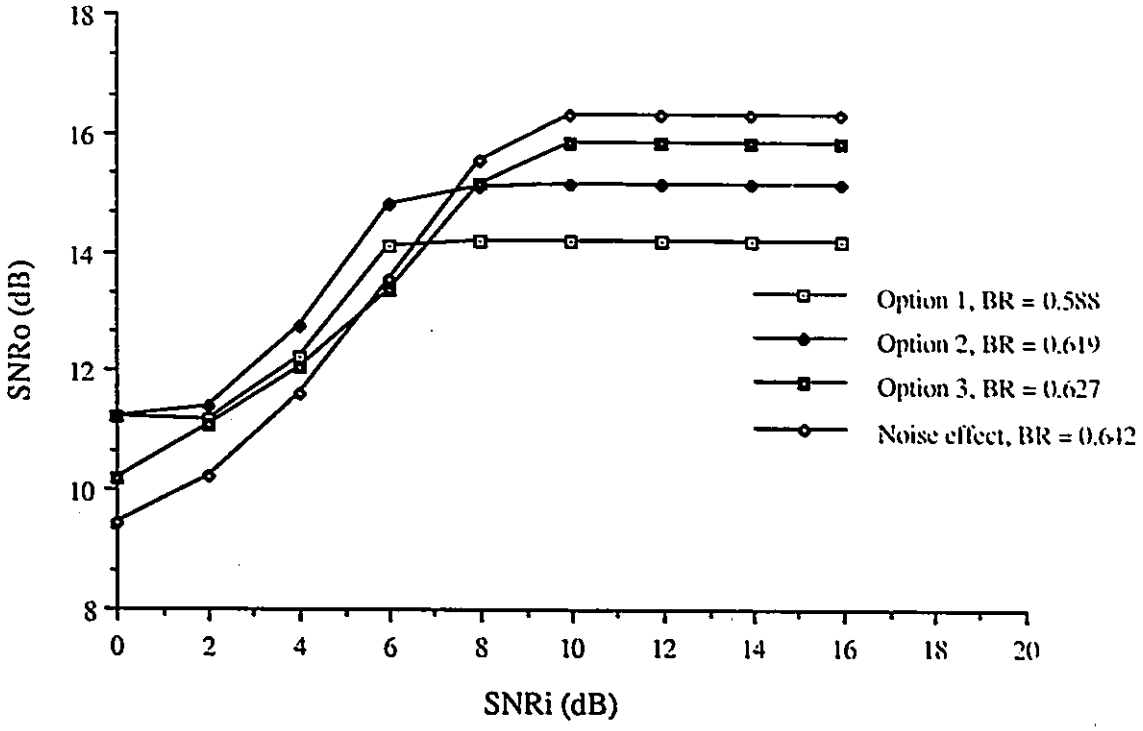

Figure 6.2: Performiance of three combined source-channel basic frame replenishment (BFR) coding schemes.

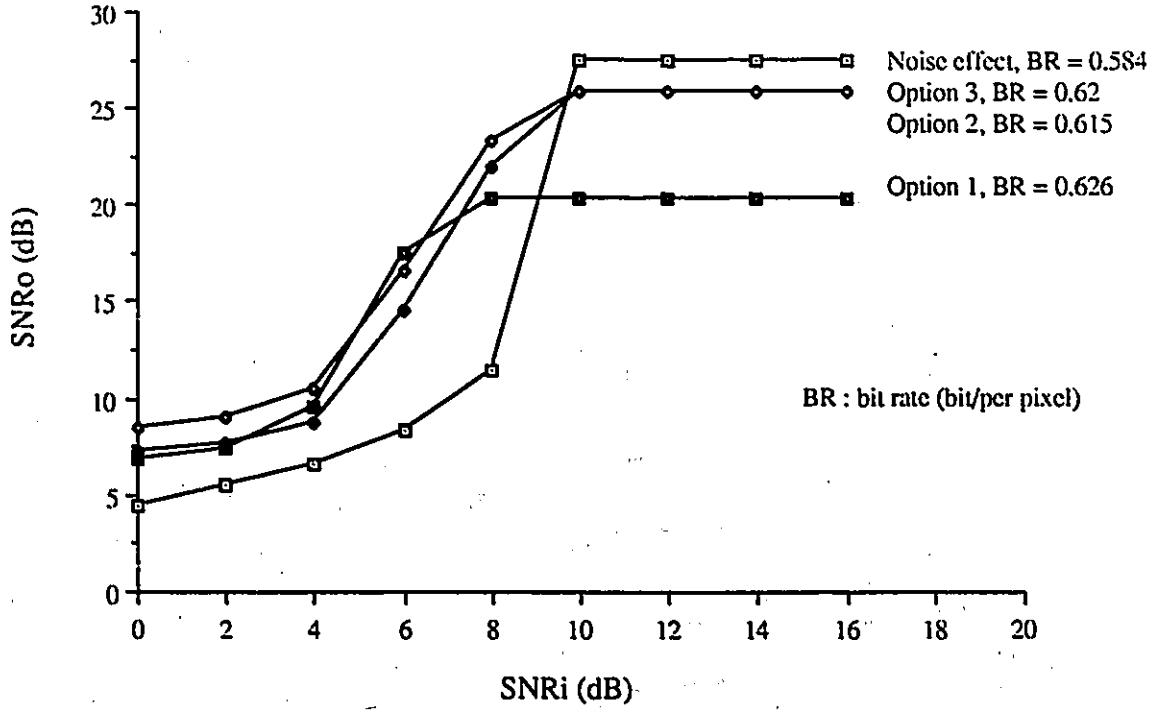

Figure 6.3: Performance of three combined source-channel label replenishment coding (LRVQ) schemes.

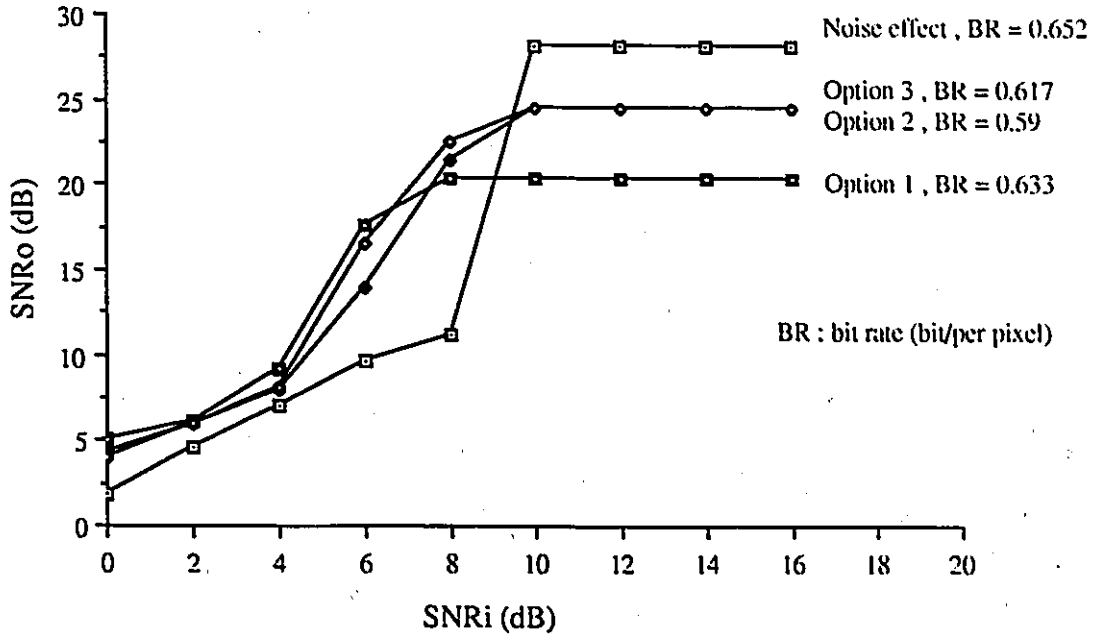

Figure 6.4: Performance of three combined source-channel codeword replenishment coding (CWRVQ) schemes.

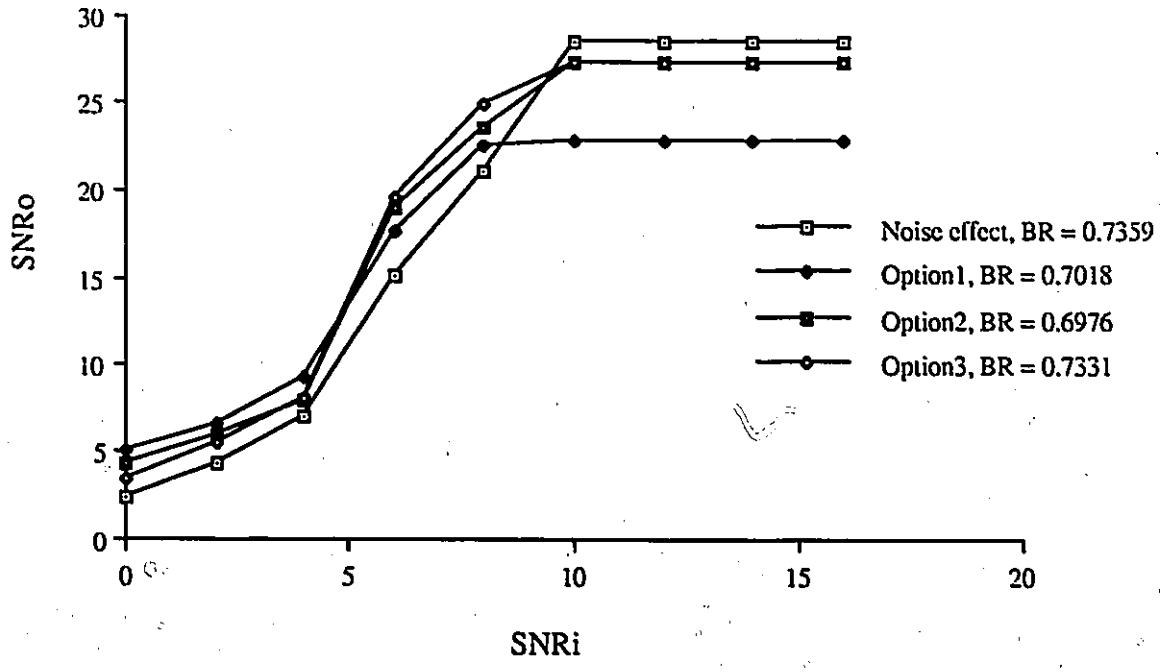

Figure 6.5: Performance of three combined source-channel label replenishment coding (LRVQ) schemes for the angiogram image sequence.

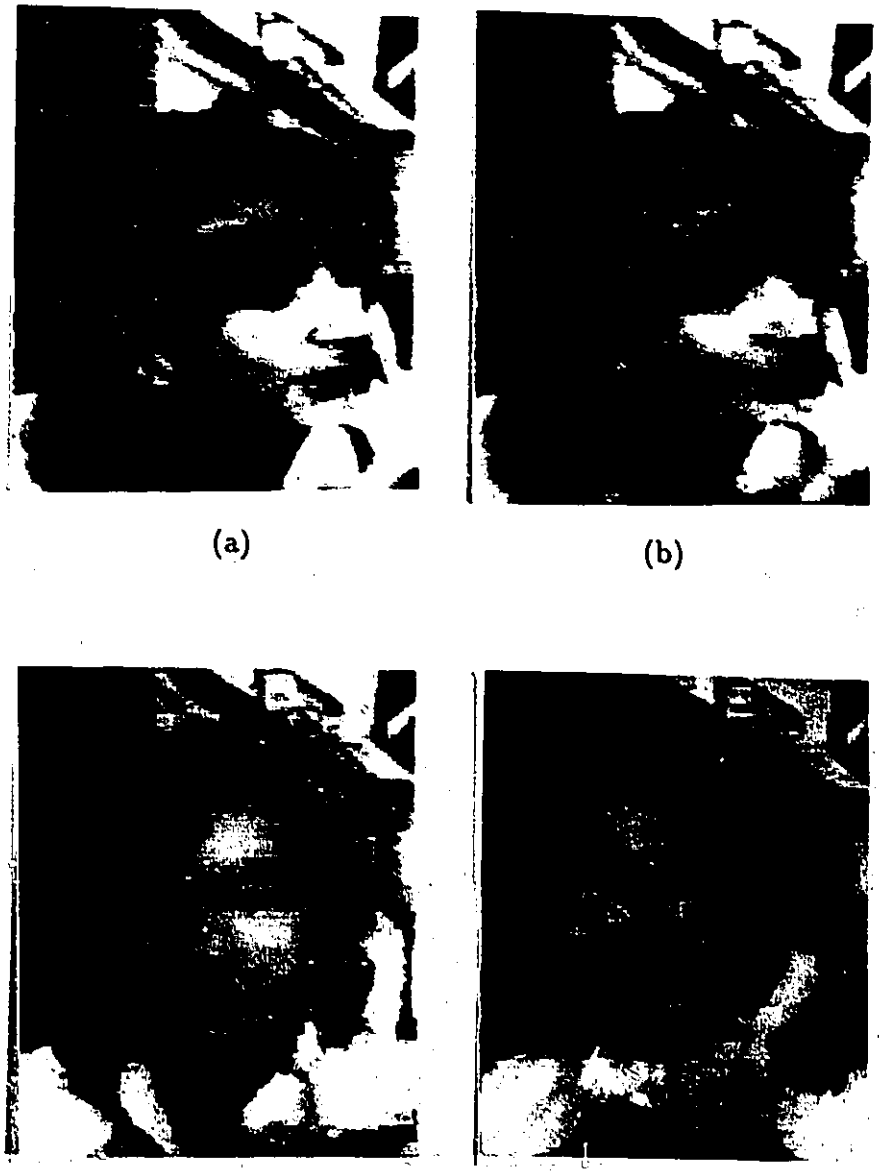

Figure 6.6: The pictorial results of combined source-channel label replenishment coding (LRVQ) with Protection 3 over SNR_i=9 dB channel: (a) the 8-th frame, (b) the 10-th frame, (c) the 15-th frame and (d) the 20-th frame.

Chapter 7

Summary and Suggestions for Future Work

7.1 Summary

In this thesis, an effort has been made to compare the performances of three frame replenishment coding schemes for noiseless and noisy channel transmission. With the help of the results obtained from the first two experiments, we propose a combined source-channel coding scheme which provides error protection in order to improve the performance over noisy channels while maintaining a fixed transmission bandwidth. The three frame replenishment coding techniques are: basic frame replenishment coding (BFR) [66], label replenishment coding using vector quantization (LRVQ) [30] and codeword replenishment coding using vector quantization (CWRVQ) [30].

Coding performance of BFR, LRVQ and CWRVQ over noiseless channels

We have simulated the three frame replenishment coding techniques over a noiseless channel. The results obtained from our experiments for the two image sequences clearly show that LRVQ and CWRVQ techniques provide significant gains in performance compared with BFR technique. This is due to the fact that BFR is more sensitive to motion in the image sequences compared with LRVQ and CWRVQ.

Coding performance of BFR, LRVQ and CWRVQ over noisy channels

Two kinds of channel error effects, error propagation and average noise effects, have been measured.

When channel errors are introduced only to the transmission of the second frame, the results on error propagation demonstrate that the efficient coding schemes LRVQ and CWRVQ are more seriourly perturbed than BFR for both image sequences i.e. with small and rapid changes. When channel errors are introduced to the transmission of the image sequences, the results on noise effects clearly show LRVQ and CWRVQ exhibit high sensitivities to channel errors, resulting in poor performance, especially when the pictures become active.

Combined source channel coding techniques

A combined source channel coding with three different error protection schemes has been proposed to improve the performance of BFR, LRVQ and CWRVQ over noisy channels, while maintaining a fixed transmission bandwidth. The simulation results demonstrate that the combined source channel coding provides significant improvement in coding performance over noisy channels without sacrificing bandwidth, especially for efficient coding techniques such as LRVQ and CWRVQ. Meanwhile, our simulation results show that for a fixed channel SNR_i the percentage of bit rate allocated to error protection should be larger for more efficient coding, LRVQ and CWRVQ than BFR, to achieve the best performance; and for a coding technique the percentage of bit rate allocated to error protection should be larger for a noisier channel.

7.2 Suggestions for Future Work

Some of the points discussed below can be considered as possible directions for future work.

1. The combined source channel coding could be made more efficient by further investegations on the tradeoffs between percentage of bit rates allocated to error protection and source coding.

2. Frame replenishment coding using vector quantization, such as LRVQ and CWRVQ could be improved over noisy channels by further studies on the codebook design by using the generalized Gray code.

3. It can be observed that when there are rapid changes in the image sequences, address method for side information transmission is better than map method; however, when there are small changes in the images, map method is better than address method. Hence, further studies have to be conducted to adapt side information to changes in image sequences.

4. Our simulation results show that the coding performance decreases rapidly when the image sequences become active. Hence, it is more important for image sequences with rapid changes to use combined source channel coding techniques in the image transmission over noisy channels, especially for efficient coding. Therefore, further investegations have to be conducted to adapt combined source channel coding schemes to changes in the image sequences.

Bibliography

[1] J. P. Adoul, C. Collin and D. Dalle, "Block encoding and its application to data compression of PCM speech," *Proc. Canadian Communications EHV Conf.* , Montreal, P. Q. , Canada, pp. 145-148, 1978.

[2] V. R. Algazi, " The psycho-physics of vision and their relation to picture quality and coding limitations," *Acta Electron.* , vol. 19, No. 3, pp. 225-232, 1976.

[3] H. C. Andrews and W. K. Pratt, " Fourier transform coding of images," *Proc. Hawaii Int. Conf. Syst. Sci.* , pp. 677-679, Jan. 1968.

[4] R. J. Arguello, " The effect of channel errors in the DPCM transmission of sampled imagery," *IEEE Trans. COMM.* , vol. COM-19, No. 6, pp. 926-933, Dec. 1971.

[5] E. Ayanoglu, "The Design of joint source and channel trellis waveform coders," *IEEE Trans. on Infor. Theory*, vol. IT-33, No. 6, pp.746-751, Nov. 1987.

[6] T. Berger, *Rate distortion theory*, Prentice-Hall, Inc, 1971.

[7] P. Boucher, " Transform image coding by vector quantization," *Neuvieme Colloque sur le traitement du signal et ses applicationa*, Gretsi Nice, pp. 629-632, May 1983.

[8] P. Boucher and M. Goldberg, " Color image compression by adaptive vector quantization, " *Proc. IEEE ICASSP*, San Diego, CA, Mar. 1984, pp. 29. 6. 1-29. 6. 4.

[9] Z. L. Budrikis, " Visual fidelity criterion and modeling ," *Proc. IEEE* , vol. 60, pp. 771-779, July 1972.

[10] J. C. Candy, M. A. Franke, " Transmitting television as clusters of frame-to-frame differences," *B. S. T. J.* , vol-50, no. 6, pp. 1889-1917, 1971.

[11] K. Y. Chang, " Analysis, optimization and sensitivity study of differential PCM systems operating on noisy communications channels," *IEEE Trans. Commun.* , vol. COM-20, pp. 338-350, June 1972.

[12] K. Y. Chang, " The effects of channel errors in DPCM systems and comparison with PCM systems ," *IEEE Trans. Commun.* , vol. COM-21, pp. 867-877, August 1973.

[13] D. T. S. Chen, "On two-or more dimensional optimum quantizers," *Proc IEEE Intl. Conf. Acoustics. , Speech, and Signal Processing*, pp. 640-643, 1977.

[14] W. H. Chen and C. H. Smith, "Adaptive coding of monochrome and color images," *IEEE Trans. Commun.*, vol. Com-25, pp. 1285-1292, Nov. 1977.

[15] N. T. Cheng, " Robust zero-redundancy vector quantization for noisy channels," in *Proc. ICC, Boston, June 1989*, pp. 1338-1342.

[16] D. J. Connor, " Intraframe coding for picture transmission ," *Proc. IEEE*, vol-60, pp. 780-791, 1972.

[17] D. J. Connor, " Techniques for reducing the visibility of transmission errors in digitally encoded video signals," *IEEE Trans. Commun*, vol. COM-21, pp. 695-706, 1973.

[18] T. N. Cornsweet, *Visual perception*. New York: Academic Press 1970.

[19] R. V. Cox and A. G. Tescher, " Generalized adaptive transform coding," *Proc. Picture Coding Symposium*, pp. 12-16, Asilomar, Calif. Jan. 1976.

[20] D. G. Daut, " Two-dimensional DPCM image transmission over fading channels," *IEEE Trans. Commun*, vol. COM-31, no. 3, pp. 315-328, March 1983.

[21] L.D. Davisson, " Rate distortion theory and application, " *Proc. IEEE*, vol. 60, pp. 800-808, July 1972.

[22] J. G. Dunham, "Joint source and channel trellis encoding," *IEEE Trans. Infor. Theory*, vol. IT-27, pp. 516-519, July 1981.

[23] M. P. Ekstrom, *Digital Image processing techniques*, Computational techniques, 1984.

[24] J. E Essman, " The effects of channel errors in DPCM systems and comparison with PCM systems," *IEEE Trans. Commun.* , vol. COM-21, no. 8, pp. 867-877, Aug. 1973.

[25] J. E. Essman, " Nonadaptive DPCM transmission of monochrome pictures over noisy communications channels," *IEEE Trans. Commun.* , vol. COM-24, pp. 173-183, February 1976.

[26] N. Farvard, "Optimal quantizer design for noisy channels: an approach to combined source-channel coding," *IEEE Trans Info. Theory*, vol. 27, no. 6, pp. 827-838, Nov. 1987.

[27] D. M. Fenwick , " Predictable sample error detector and a planar prediction corrector for removal of isolated transmission errors in Walsh-Hadamard transformed pictures," *Electron. Lett.* , vol. 13, pp. 8-10, Jan. 6, 1977.

[28] A. Gersho, " On the structure of vector quantizer," *IEEE Trans. on Commun.* , vol. Com-29, no. 12, pp. 1809-1817, Dec. 1981.

[29] A. Gersho, "Asymptotically optimum block quantizers," *IEEE Trans. Inform. Theory.* , vol. IT-25, pp. 373-380, July 1979.

[30] M. Goldberg and H. F. Sun, " Image sequence coding using vector quantization," *IEEE Trans. Commun.* , vol. COM-34, pp. 703-710, July, 1986.

[31] R. C. Gonzalez and P. Wintz, *Digital image processing*, Addison-Wesley, 1987.

[32] D. J. Goodman, " Transmission errors and forward error correction in embedded DPCM," *B. S. T. J.* , vol. 62, no. 9, pp. 145-152, Nov. 1983.

[33] D. J. Goodman, "Combined source and channel coding for variable-bit-rate speech transmission," *Bell Syst. Tech. J.* , vol. 62, pp. 2017-2036, Sept. 1983.

[34] R. M. Gray, "Vector quantization," *IEEE ASSP Mag.* , pp. 4-29, April 1984.

[35] A. Habibi, " Hybrid coding of pictorial data," *IEEE Trans. Infor. Theory*, vol. com-22, No. 5, pp. 614-624, May, 1974.

[36] A. Habibi, " Survey of adaptive image coding techniques," *IEEE Trans. Infor. Theory*, vol. com-25, No. 11, pp. 1275-1284, Nov. 1977.

[37] E. L. Hall, *Computer image processing and recognition*, Academic Press, New York, 1979.

[38] B. G. Haskell, F. W. Mounts and J. C. Candy, " Interframe coding of video-telephone pictures, " *Proc. IEEE*, no. 60, pp. 792-800, July 1972.

[39] M. E. Hellman, "Convolutional source encoding," *IEEE Trans. Infor. Theory*, vol. IT-21, No. 6, pp. 651-656, Nov. 1975.

[40] T. S. Huang , "Run-length coding and its extensions, " *Picture Bandwidth Compression* , Gordon and Breach, New York, 1972.

[41] T. S. Huang and M. T. Chikhaoui, "The effect of BSC on PCM picture quality," *IEEE Trans. Inf. Theory*, IT-13, 2, pp. 270-273, April, 1967.

[42] T. S. Huang and R. Y. Tsai, "Image sequence analysis: motion estimation," *Image Sequence Analysis*, T. S. Huang (Editor), pp. 1-17, 1980.

[43] D. Huffman, "A method for the construction of minimum redundancy codes, " *Proc. IRE*, pp. 1098-1101, April, 1967.

[44] T. Ishiguro, K. Iinuma, " Robust zero-redundancy vector quantization for noisy channels," in *Natl. Telecommun. Conf. Rec.* , , Vol. 1, pp. 6. 4-1 to 6. 4-5.1976

[45] J. R. Jain and A. K. Jain, "Displacement measurement and its applications in interframe coding, " *IEEE Trans. on Commun.* ; vol. Com-29, pp. 1799-1806, Dec. 1981.

[46] A. K. Jain, "Image data compression: A review," *IEEE Proceeding*, vol. 69, pp. 349-389, March 1981.

[47] N. S. Jayant and P. C. Noll, *Digital coding of waveform*, Prentice-Hall, 1984.

[48] D. H. Kelly, "Effects of sharp edges on the visibility of sinusoidal gratings," *J. Opt. Soc. Amer.*, vol. 60, pp. 98-103, Jan. 1970.

[49] N. M. Nasrabadi and R. A. King, "A new image coding technique using transforms vector quantization," *IEEE Proc. ICASSP*, pp. 29.9.1-29.9.4, 1984.

[50] J. M. Knight, "Maximum acceptable bit error rates for PCM analog and digital TV systems," *Proceedings National Telemetering Conference*, pp. 1-9, 1962.

[51] T. Koga, K. Iinuma, "Motion compensated interframe image coding for video conferencing," *NTC 81, Proc. Ing*, pp. G5. 3. 1-G5. 3. 5, New Orleans, LA, Dec. 1981.

[52] V. N. Koshelev, "Direct sequential encoding and decoding for discrete sources," *IEEE Trans. Infor. Theory*, vol. IT-19, no. 3 , pp. 340-343, May, 1973.

[53] H. Kumazawa, " A construction of vector quantizers for noise channels," *Electronic and Engineering in Japan*, vol. 67-B, no. 4, pp. 1-8, 1984.

[54] A. J. Kurtenbach, "Quantizing for noisy channels," *IEEE Trans. Comm. Tech.*, vol. 17, no. 2, pp. 291-302, Apr. 1969.

[55] K. J. Larsen, " Short convolutional codes with maximal free distance for rate 1/2, 1/3, and 1/4," *IEEE Trans. Inform. Theory*, vol. IT-19, pp. 371-373, May 1973.

[56] K-H Lee, " Optimal linear coding for vector channels," *IEEE Trans. Commun.*, vol. COM-24, no. 12, pp. 1283-1290, Dec. 1976.

[57] J. O. Limb and R. F. W. Pease, "A simple interframe coder for video telephony," *B. S. T. J.*, no. 50, pp. 1877-1888, Aug. 1971.

[58] S. Lin and D.J. Costello, *Error control coding - fundemantals and applications*, Academic Press, 1985.

[59] Linde, " An algorithm for vector quantizer design," *IEEE Transactions on ASSP*, vol. ASSP-28, no. 5 pp. 562-574, Oct. 1980.

[60] S. P. Lloyd, "Least squares optimization in PCM," *IEEE Trans. Inform. Theory.*, vol. IT-28, pp. 129-137, March 1982.

[61] J. L. Mannos and D. J. Sakrison, " The effects of a visual fidelity criterion on the encoding of images," *IEEE Trans. Inform. Theory*, vol. IT-20, pp. 525-236, July 1974.

[62] H. Meyr, H. G. Rosdolsky and T. S. Huang, "Optimum run-length codes," *IEEE Trans. on Communications*, pp. 826-835, June 1974.

[63] J. W. Modestino and D. Daut, " Combined source-channel coding of images," *IEEE Trans. Commun.*, vol. COM-27, pp. 1644-1659, Nov. 1979.

[64] J. W. Modestino and D. Daut, " Combined source-channel coding of images using the block cosine transform," *IEEE Trans. Commun.* , vol. COM-29, pp. 1261-1271, September 1981.

[65] J. W. Modestino and D. Daut, "Tree encoding of images in the presence of channel errors," *IEEE Trans Inform. Theory*, vol. 27, pp. 677-697, Nov. 1981.

[66] W. F. Mounts, "A video encoding system using conditional picture element replenishment," *B. S. T. J.* , no. 7, pp. 2545-2554, Sept. 1969.

[67] K. N. Nagn, "Enhancement of PCM and DPCM images corrupted by transmission errors," *IEEE Trans. Commun*, vol. COM-30, pp. 257-265, 1982.

[68] A. N. Netravali, "Picture coding: a review," *IEEE Proceeding*, vol. 68, No. 3, pp. 366-407, March 1980.

[69] A. N. Netravali and J. D. Robbins, "Motion compensated television coding-part I," *B.S.T.J.*, pp. 631-670, March 1979.

[70] A. N. Netravali and B. Prasada, "Adaptive quantization of picture signals using spatial masking," *IEEE Proceeding*, vol. 65, pp. 536-548, April 1977.

[71] Y. Ninomiya and Y. Ohtsuka, " A motion-compensated interframe coding scheme for television pictures," *IEEE Trans. Commun*, vol. Com-30, pp. 201-211, Jan. 1982.

[72] P. Noll, " On predictive quantizing schemes," *B. S. T. J.* , May-June, 1978, pp. 1499-1532.

[73] J. P. Odenwalder, " Optimal decoding of convolutional codes, " Ph. D. dissertation, School Eng. and Appl. Science, University of California, Los Angeles, 1970.

[74] R. F. W. Pease and J. O. Limb, " Exchange of spatial and temporal resolution in television coding," *B. S. T. J.* , vol. 50, pp. 191-200, Jan. 1971.

[75] W. K. Pratt, *Image transmission techniques*, Academic Press, N. Y. , 1979.

[76] W. K. Pratt, *Digital image processing*, Academic Press, N. Y. , 1977.

[77] W. K. Pratt, J. Kane and A. C. Andrews, " Hadamard transform image coding," , *Proc. of IEEE* , vol. 75, pp. 58-68, Jan. 1969.

[78] J.G. Proakis, *Digital communications (second edition)*, McGraw-Hill, 1989.

[79] J. A. Roese, W. K. Pratt, J. Kane and G. S. Robinson, " Interframe cosine transform image coding," , *IEEE Trans. on Commun.*, vol. 25, pp. 1329-1339, Nov. 1977.

[80] A. Rosenfeld and A. C. Kak, *Digital picture processing*, Academic Press, New York, 1982.

[81] N. Rydbeck, " Analysis of digital errors in nonlinear PCM systems," *IEEE Trans. Commun.* , vol. COM-24, no. 1, pp. 59-65, Jan. 1976.

[82] C. E. Shannon, " A mathematical theory of communication, " *B. S. T. J.* , vol. 27, pp. 379-423, 623-656, 1948.

[83] R. Steele, D. J. Goodman and C. A. McGonegal, " A difference detection and correction scheme for combating DPCM transmission errors," *IEEE Trans. Commun.* , vol. COM-27, no. 1. pp. 321-326, Jan. 1979.

[84] R. Steele, " DPCM with force updating and partial correction of transmission errors," *B. S. T. J.* , vol. 58, no. 3, pp. 721-728, March 1979.

[85] R. Steele and D. J. Goodman, " Adaptive difference detection and correction system for partial correction of transmission errors in linear PCM," *B. S. T. J.* , vol. 14, no. 12, pp. 381-382, June 1978.

[86] R. Steele and D. J. Goodman, "Partial correction of transmission errors in DPCM without recourse to error correction coding," *Electron. Lett.* , vol. 13, pp. 351-353, June 1977.

[87] R. Steele and D. J. Goodman, " Detection and selective smoothing of transmission errors in linear PCM," *B. S. T. J.* , vol. 56, no. 3, pp. 399-409, March 1977.

[88] H. F. Sun and M. Goldberg, " Adaptive vector quantization for image sequence coding, " *Proc. IEEE ICASSP*, pp. 339-342, Tampa, FL, Mar. 1985.

[89] H. F. Sun, Interfrmae image coding by adaptive Vector quantization, *Ph. D Thesis*, March 1986.

[90] N. Tanabe and N. Farvardin, "Subband image coding using entropy-coded quantization over noisy channel," *ICASSP*, pp. 78-84, Feb. 1990.

[91] M. Tasto and P. A. Wintz, "Image coding by adaptive block quantization," *IEEE Trans. Commun.* , vol. COM-19, pp. 957-972, Dec. 1971.

[92] R. E. Totty, "Reconstruction error in waveform transmission," *IEEE Trans. Inform. Theory*, vol. IT-13, pp. 336-338, April 1967.

[93] J. Tou, *Pattern recognition principles*, Addison-Wesley Publication Company, 1974.

[94] P. A. Wintz, " Transform picture coding ," *Proc. IEEE* , vol. 60, pp. 809-820, July 1972.

[95] W. C. Wong and R. Steele, " Partial correction of transmission errors in Walsh transform image without recourse to error correction coding," *Eletron. Lett.* , vol. 14, pp. 298-300, May 1978.

[96] A. J. Viterbi, "Convolutional codes and their performance in communication systems," *IEEE Trans. Commun.*, vol. COM-19, pp. 751-772, Oct. 1971.

[97] H. Yasuda, " 1.544 Mbits/s transmission of TV signals by interframe coding systems," *IEEE Trans. Commun.* , vol. COM-24, pp. 1175-1180, Jan. 1976.

[98] R. Zelinski, " Effects of transmission errors on the mean-squared error performance of transform coding system," *IEEE Trans. Acoust. , Speech, Signal Processing*, vol. 27, no. 5, pp. 531-537, Oct. 1979.

[99] J. Zdepski, " Noisy channel performance of intraframe VQ coding of images," *Proc. IEEE*, vol. 3, pp. 1240-1244, Philadelphia, June 1988.

[100] K. A. Zege and A. Gersho, " Zero redundancy channel coding in vector quantization," *Electri. Letters*, vo. 123, No. 12, pp. 654-656, June 1987.

[101] K. A. Zeger and A. Gersho, " Vector quantizer design for memoryless noisy channels," in *Procedings of IEEE Inter. Confer. on Comm.* , vol. 3, pp. 1593-1597, June, 1988.